Instrumentation in HEP

EIROFORUM School of Instrumentation

June 16 2015

Werner Riegler, CERN, werner.riegler@cern.ch

Creation of the Signal

Charged particles traversing matter leave excited atoms, electron-ion pairs (gases) or electrons-hole pairs (solids) behind.

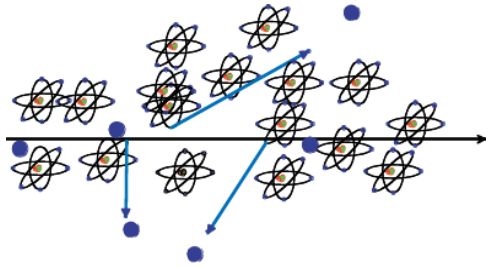

Excitation:

The photons emitted by the excited atoms in transparent materials can be detected with photon detectors like photomultipliers or semiconductor photon detectors.

Ionization:

By applying an electric field in the detector volume, the ionization electrons and ions are moving, which induces signals on metal electrodes. These signals are then read out by appropriate readout electronics.

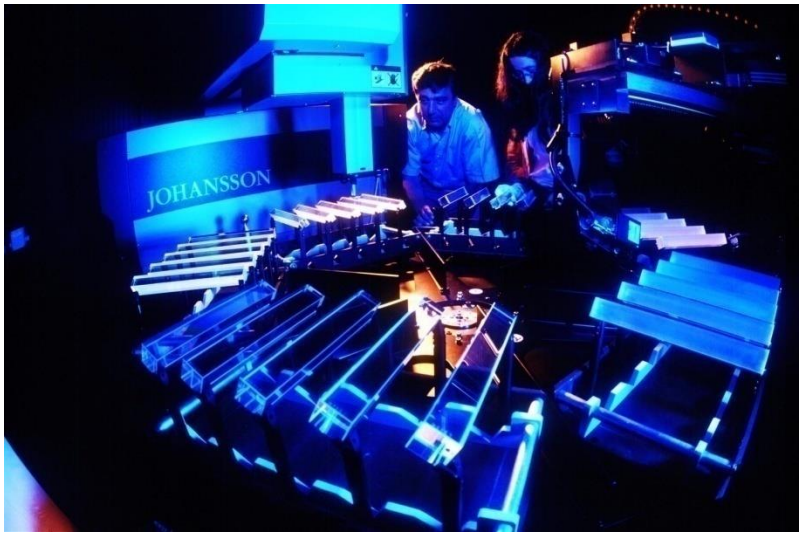

Detectors based on registration of excited Atoms → Scintillators

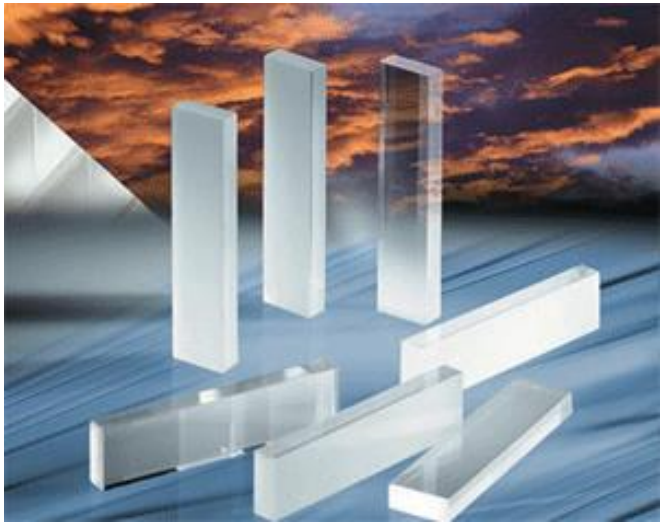

Detectors based on Registration of excited Atoms → Scintillators

Emission of photons of by excited Atoms, typically UV to visible light.

a) Observed in Noble Gases (even liquid !)

b) Inorganic Crystals

→ Substances with largest light yield. Used for precision measurement of energetic Photons. Used in Nuclear Medicine.

c) Polyzyclic Hydrocarbons (Naphtalen, Anthrazen, organic Scintillators)

→ Most important category. Large scale industrial production, mechanically and chemically quite robust. Characteristic are one or two decay times of the light emission.

Typical light yield of scintillators:

Energy (visible photons) ≈ few % of the total energy Loss.
z.B. 1cm plastic scintillator, ρ ≈ 1, dE/dx=1.5 MeV, ~15 keV in photons;
i.e. ~ 15 000 photons produced.

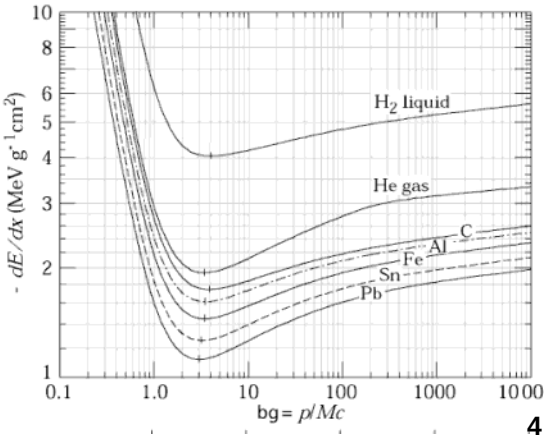

Detectors based on Registration of excited Atoms → Scintillators

Organic ('Plastic') Scintillators

Low Light Yield

Fast: 1-3ns

Type	Light output[a]	λ_{max}[b] (nm)	Attenuation length (cm)	Risetime (ns)	Decay time (ns)	Pulse FWHM (ns)
NE 102A	58–70	423	250	0.9	2.2–2.5	2.7–3.2
NE 104	68	406	120	0.6–0.7	1.7–2.0	2.2–2.5
NE 104B	59	406	120	1	3.0	3
NE 110	60	434	400	1.0	2.9–3.3	4.2
NE 111	40–55	375	8	0.13–0.4	1.3–1.7	1.2–1.6
NE 114	42–50	434	350–400	~1.0	4.0	5.3
Pilot B	60–68	408	125	0.7	1.6–1.9	2.4–2.7
Pilot F	64	425	300	0.9	2.1	3.0–3.3
Pilot U	58–67	391	100–140	0.5	1.4–1.5	1.2–1.9
BC 404	68	408	—	0.7	1.8	2.2
BC 408	64	425	—	0.9	2.1	~2.5
BC 420	64	391	—	0.5	1.5	1.3
ND 100	60	434	400	—	3.3	3.3
ND 120	65	423	250	—	2.4	2.7
ND 160	68	408	125	—	1.8	2.7

LHC bunchcrossing 25ns

Inorganic (Crystal) Scintillators

Large Light Yield

Slow: few 100ns

	Relative light output	λ_{max} emission (nm)	Decay time (ns)	Density (g/cm³)
Inorganic crystals				
NaI(Tl)	230	415	230	3.67
CsI(Tl)	250	560	900	4.51
$Bi_4Ge_3O_{12}$ (BGO)	23–86	480	300	7.13
Organic crystals				
Anthracene	100	448	22	1.25
Trans-stilbene	75	384	4.5	1.16
Naphthalene	32	330–348	76–96	1.03
p,p'-Quarterphenyl	94	437	7.5	1.20
Primary activators				
2,5-Diphenyl-oxazole (PPO)	75	360–416	5[a]	
2-Phenyl-5-(4-biphenylyl)-1,3,4-oxadiazole (PBD)	96	360–5		
4,4"-Bis(2-butyloctyloxy)-*p*-quaterphenyl (BIBUQ)	60	365,393	1.30[b]	

LEP bunchcrossing 25μs

Scintillators

Photons are being reflected towards the ends of the scintillator.

A light guide brings the photons to the Photomultipliers where the photons are converted to an electrical signal.

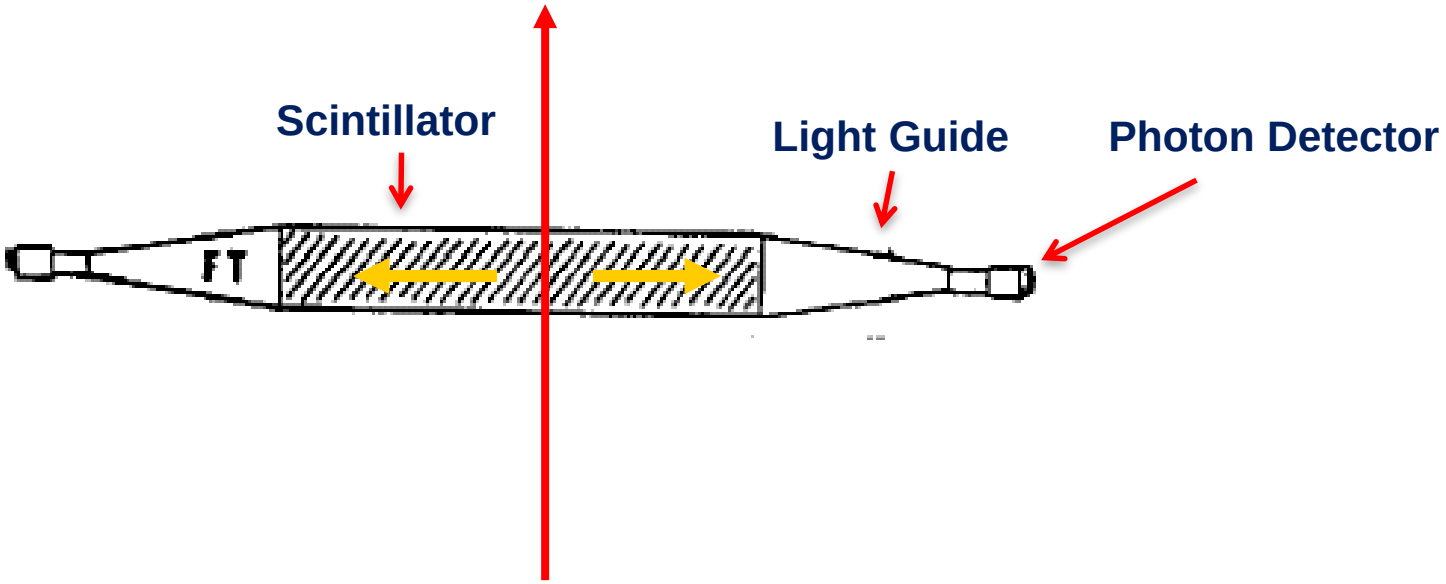

By segmentation one can arrive at spatial resolution.

Because of the excellent timing properties (<1ns) the arrival time, or time of flight, can be measured very accurately → Trigger, Time of Flight.

Typical Geometries:

- Light guides: transfer by total internal reflection (+outer reflector)

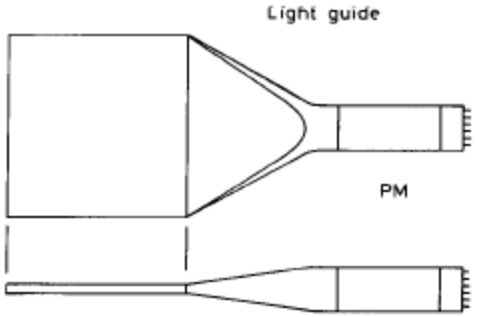

"fish tail"

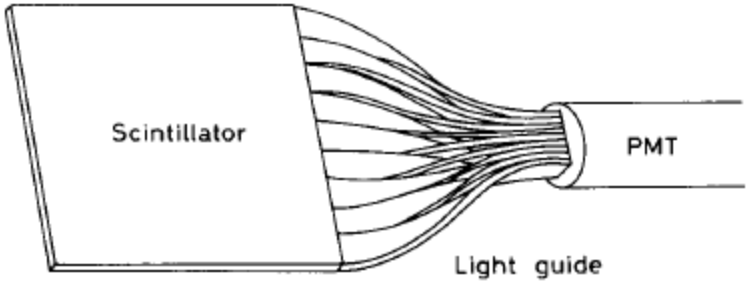

adiabatic

- wavelength shifter (WLS) bars

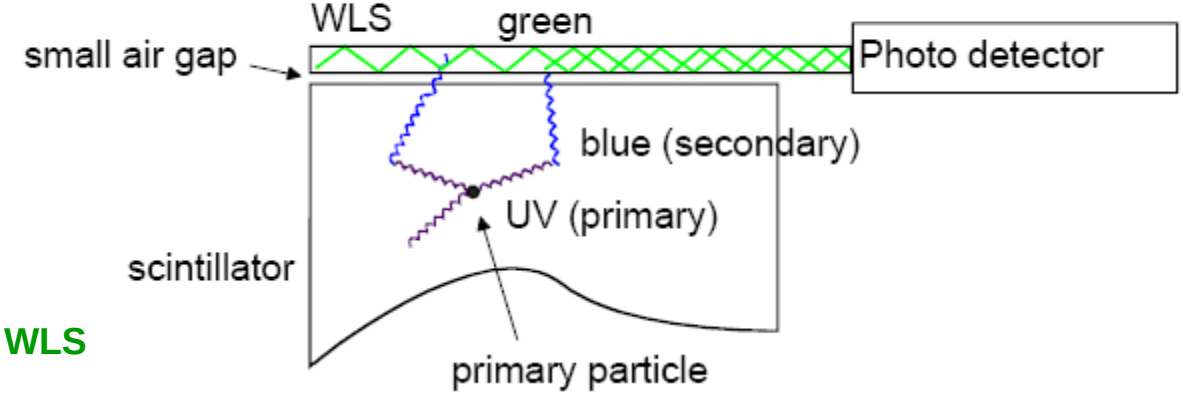

UV light enters the WLS material
Light is transformed into longer wavelength
→Total internal reflection inside the WLS material
→ 'transport' of the light to the photo detector

From C. Joram

The frequent use of Scintillators is due to:

Well established and cheap techniques to register Photons → Photomultipliers and the fast response time → 1 to 100ns

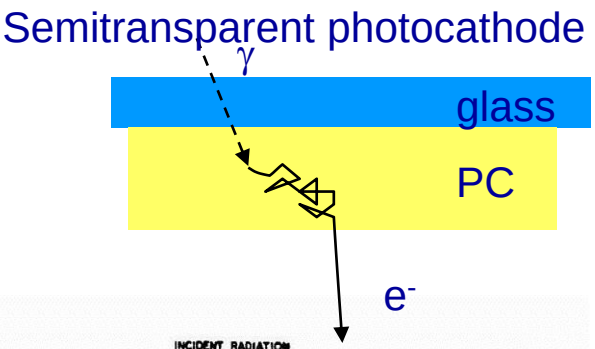

Schematic of a Photomultiplier:

- **Typical Gains (as a function of the applied voltage): 10^8 to 10^{10}**
- **Typical efficiency for photon detection:**
- **< 20%**
- **For very good PMs: registration of single photons possible.**
- **Example: 10 primary Elektrons, Gain 10^7→ 10^8 electrons in the end in T ≈ 10ns. I=Q/T = 10^8*1.603*10^{-19}/10*10^{-9}= 1.6mA.**
- **Across a 50 Ω Resistor → U=R*I= 80mV.**

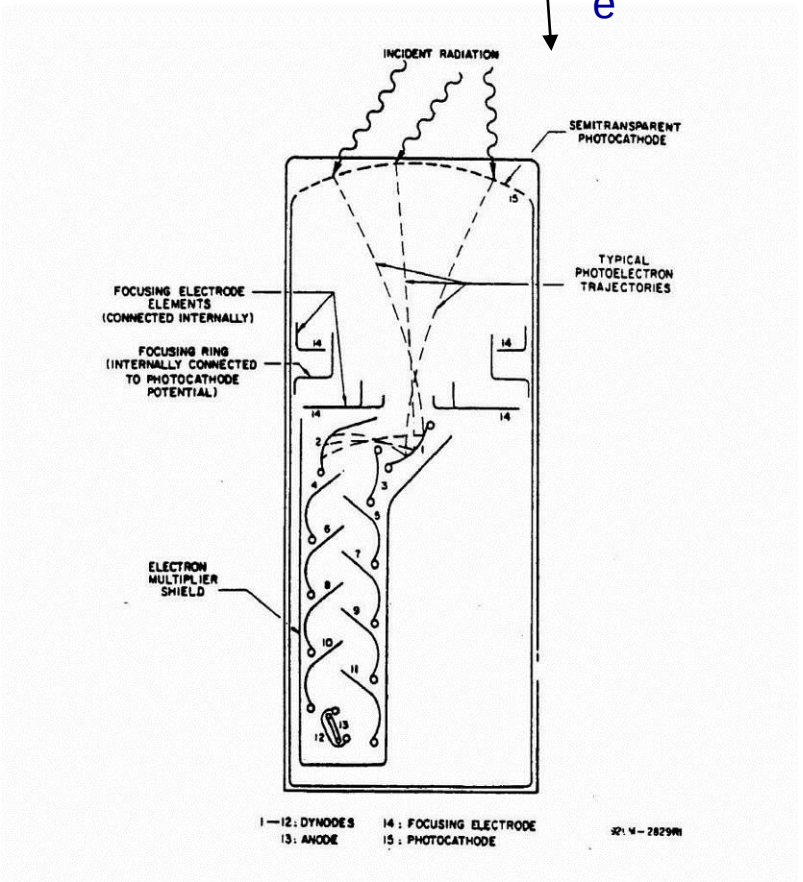

Fiber Tracking

Light transport by total internal reflection

Planar geometries
(end cap)

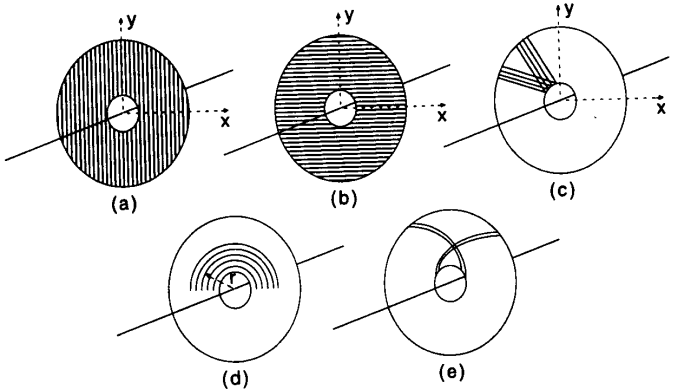

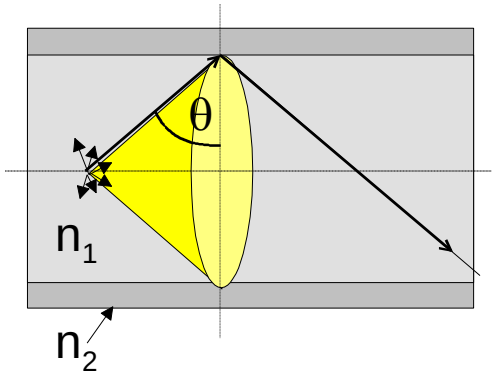

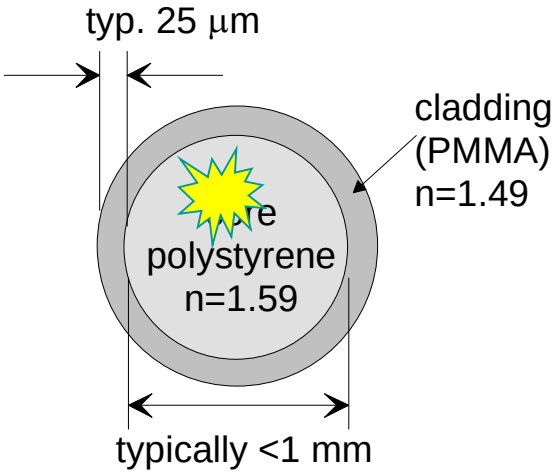

Circular geometries
(barrel)

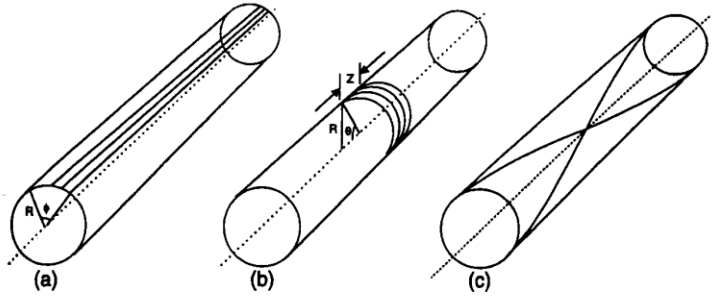

(R.C. Ruchti, Annu. Rev. Nucl. Sci. 1996, 46,281)

High geometrical flexibility

Fine granularity

Low mass

Fast response (ns)

From C. Joram

Detectors based on Registration of Ionization: Tracking in Gas and Solid State Detectors

Charged particles leave a trail of ions (and excited atoms) along their path: Electron-Ion pairs in gases and liquids, electron hole pairs in solids.

The produced charges can be registered → Position measurement → Tracking Detectors.

Cloud Chamber: Charges create drops → photography.
Bubble Chamber: Charges create bubbles → photography.
Emulsion: Charges 'blacked' the film.

Gas and Solid State Detectors: Moving Charges (electric fields) induce electronic signals on metallic electrons that can be read by dedicated electronics.

→In solid state detectors the charge created by the incoming particle is sufficient.

→In gas detectors (e.g. wire chamber) the charges are internally multiplied in order to provide a measurable signal.

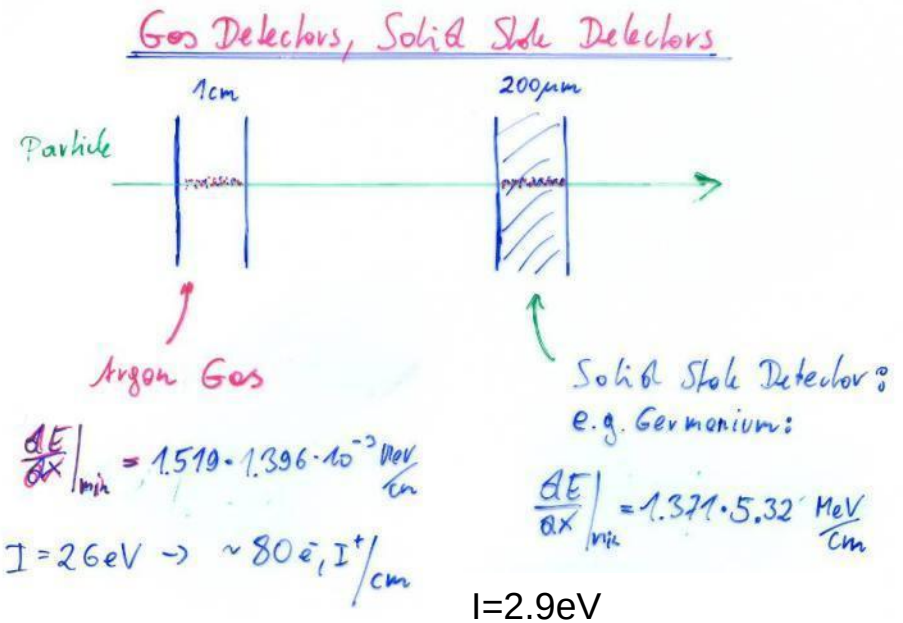

I=2.9eV
2.5 x 10^6 e/h pairs/cm

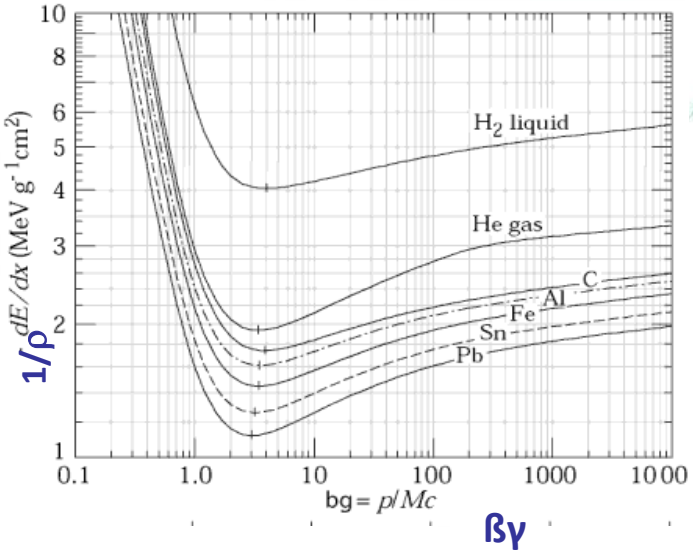

The induced signals are readout out by dedicated electronics.

The noise of an amplifier determines whether the signal can be registered. Signal/Noise >>1

The noise is characterized by the 'Equivalent Noise Charge (ENC)' = Charge signal at the input that produced an output signal equal to the noise.

ENC of very good amplifiers can be as low as 50e-, typical numbers are ~ 1000e-.

In order to register a signal, the registered charge must be q >> ENC i.e. typically q>>1000e-.

Gas Detector: q=80e- /cm → too small.

Solid state detectors have 1000x more density and factor 5-10 less ionization energy.
→Primary charge is 10^4-10^5 times larger than is gases.

Gas detectors need internal amplification in order to be sensitive to single particle tracks.

Without internal amplification they can only be used for a large number of particles that arrive at the same time (ionization chamber).

Principle of Signal Induction by Moving Charges

A point charge q at a distance z_0

Above a grounded metal plate 'induces' a surface charge.

The total induced charge on the surface is –q.

Different positions of the charge result in different charge distributions.

The total induced charge stays –q.

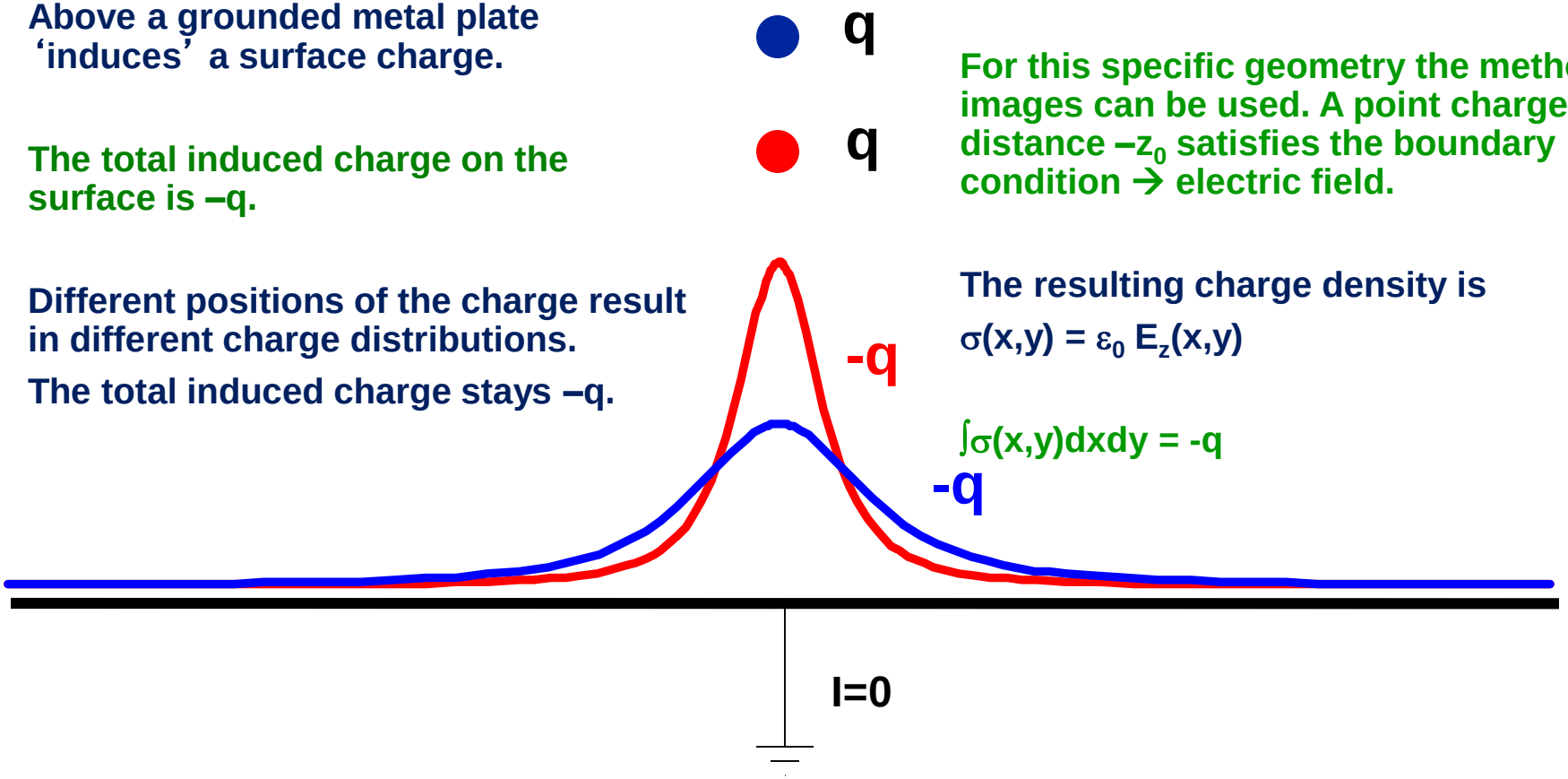

The electric field of the charge must be calculated with the boundary condition that the potential φ=0 at z=0.

For this specific geometry the method of images can be used. A point charge –q at distance $-z_0$ satisfies the boundary condition → electric field.

The resulting charge density is

$\sigma(x,y) = \varepsilon_0 E_z(x,y)$

$\int\sigma(x,y)dxdy = -q$

$$E_z(x,y) = -\frac{qz_0}{2\pi\varepsilon_0(x^2+y^2+z_0^2)^{\frac{3}{2}}} \qquad E_x = E_y = 0 \qquad \sigma(x,y) = \varepsilon_0 E_z(x,y) \qquad Q = \int_{-\infty}^{\infty}\int_{-\infty}^{\infty}\sigma(x,y)dxdy = -q$$

Principle of Signal Induction by Moving Charges

If we segment the grounded metal plate and if we ground the individual strips the surface charge density doesn't change with respect to the continuous metal plate.

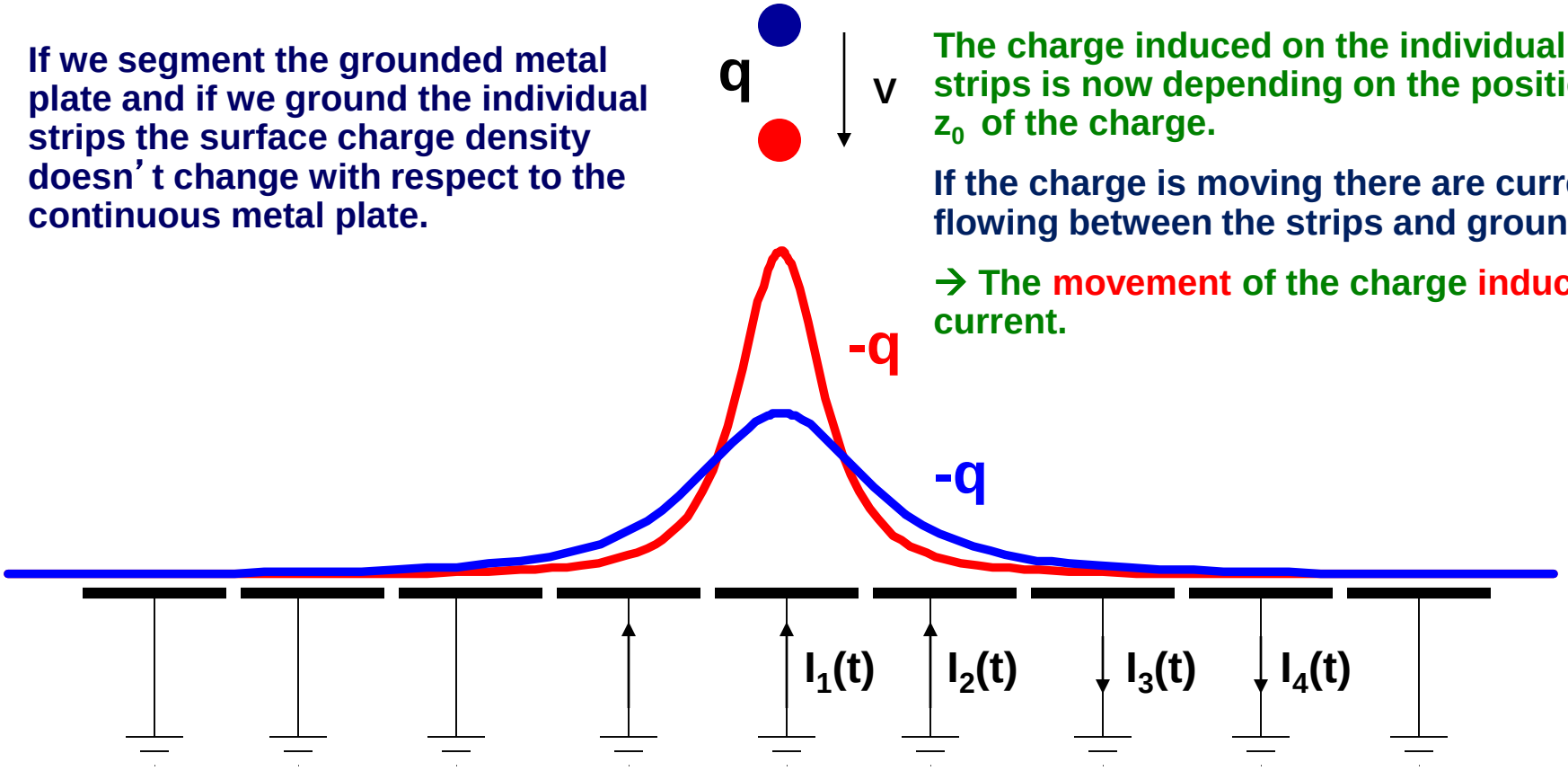

The charge induced on the individual strips is now depending on the position z_0 of the charge.

If the charge is moving there are currents flowing between the strips and ground.

→ The movement of the charge induces a current.

$$Q_1(z_0) = \int_{-\infty}^{\infty}\int_{-w/2}^{w/2} \sigma(x,y)dxdy = -\frac{2q}{\pi}\arctan\left(\frac{w}{2z_0}\right)$$

$$z_0(t) = z_0 - vt$$

$$I_1^{ind}(t) = -\frac{d}{dt}Q_1[z_0(t)] = -\frac{\partial Q_1[z_0(t)]}{\partial z_0}\frac{dz_0(t)}{dt} = \frac{4qw}{\pi[4z_0(t)^2 + w^2]}v$$

Gas Detectors with internal Electron Multiplication

Principle: At sufficiently high electric fields (100kV/cm) the electrons gain energy in excess of the ionization energy → secondary ionzation etc. etc.

$dN = N \alpha \, dx$ α…Townsend Coefficient

$N(x) = N_0 \exp(\alpha x)$ $N/N_0 = A$ (Amplification, Gas Gain)

Avalanche in a homogeneous field:

Problem: High field on electrode surface → breakdown

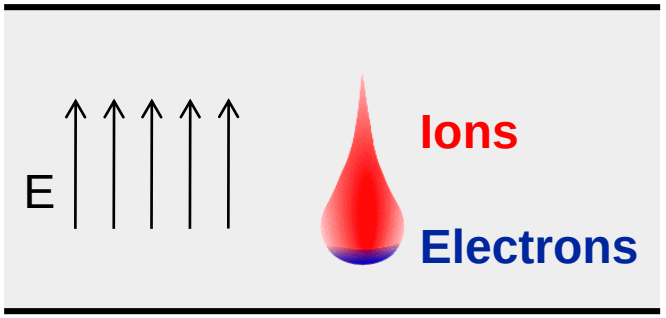

In an inhomogeneous Field: $\alpha(E)$ → $N(x) = N_0 \exp[\int \alpha(E(x'))dx']$

Wire Chamber: Electron Avalanche

Wire with radius (10-25μm) in a tube of radius b (1-3cm):

$$E(r) = \frac{\lambda}{2\pi\varepsilon_0}\frac{1}{r} = \frac{V_0}{\ln\frac{b}{a}}\frac{1}{r}, \qquad V(r) = \frac{V_0}{\ln\frac{b}{a}}\ln\frac{r}{a},$$

Electric field close to a thin wire (100-300kV/cm). E.g. V_0=1000V, a=10μm, b=10mm, E(a)=150kV/cm

Electric field is sufficient to accelerate electrons to energies which are sufficient to produce secondary ionization → electron avalanche → signal.

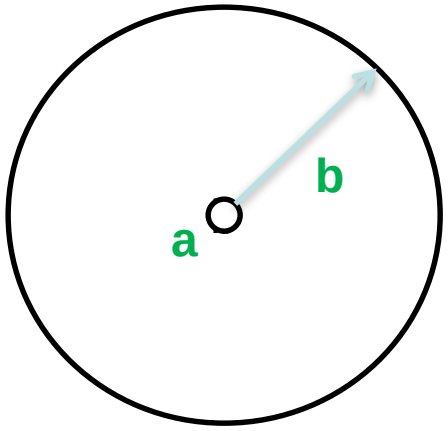

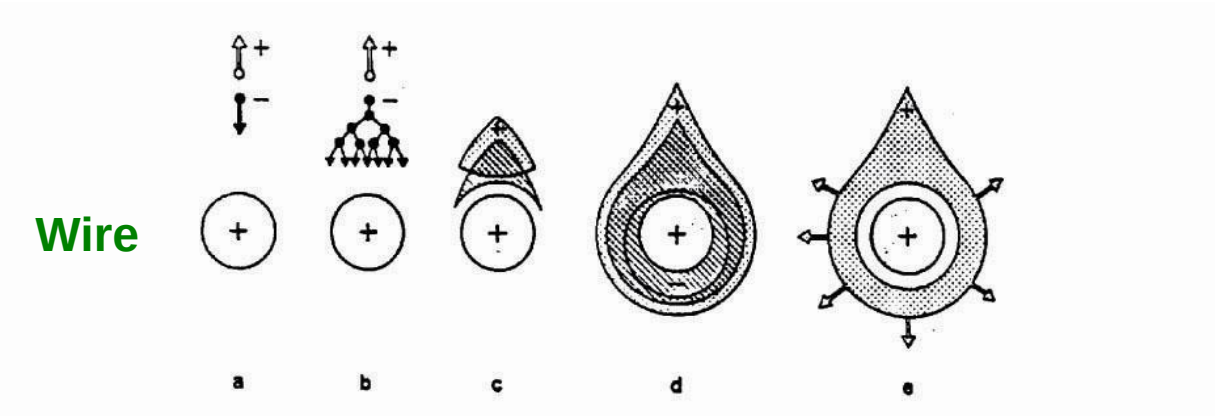

Wire Chamber: Electron Avalanches on the Wire

Proportional region: $A \approx 10^3\text{-}10^4$ — **LHC**

Semi proportional region: $A \approx 10^4\text{-}10^5$
(space charge effect)

Saturation region: $A > 10^6$
Independent the number of primary electrons.

Streamer region: $A > 10^7$
Avalanche along the particle track.

Limited Geiger region:
Avalanche propagated by UV photons.

Geiger region: $A \approx 10^9$
Avalanche along the entire wire.

1970ies

1950ies

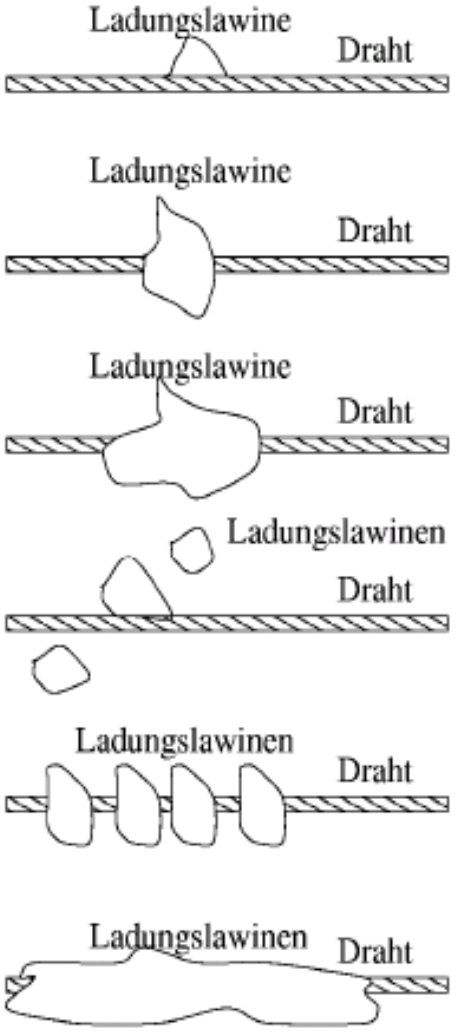

Wire Chamber: Signals from Electron Avalanches

The electron avalanche happens very close to the wire. First multiplication only around R =2x wire radius. Electrons are moving to the wire surface very quickly (<<1ns). Ions are difting towards the tube wall (typically several 100μs.)

The signal is characterized by a very fast 'spike' from the electrons and a long Ion tail.

The total charge induced by the electrons, i.e. the charge of the current spike due to the short electron movement amounts to 1-2% of the total induced charge.

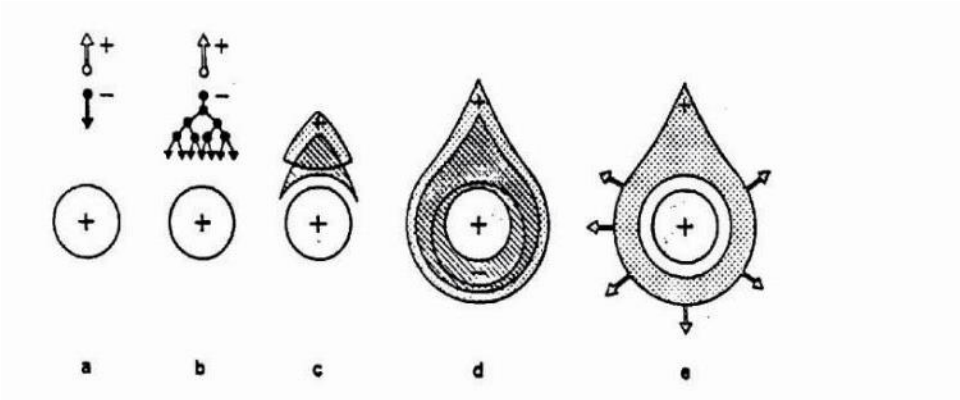

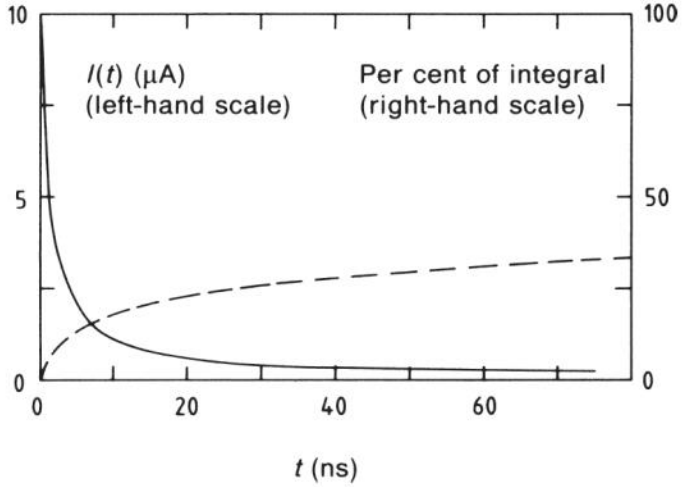

Detectors with Electron Multiplication

Rossi 1930: Coincidence circuit for n tubes

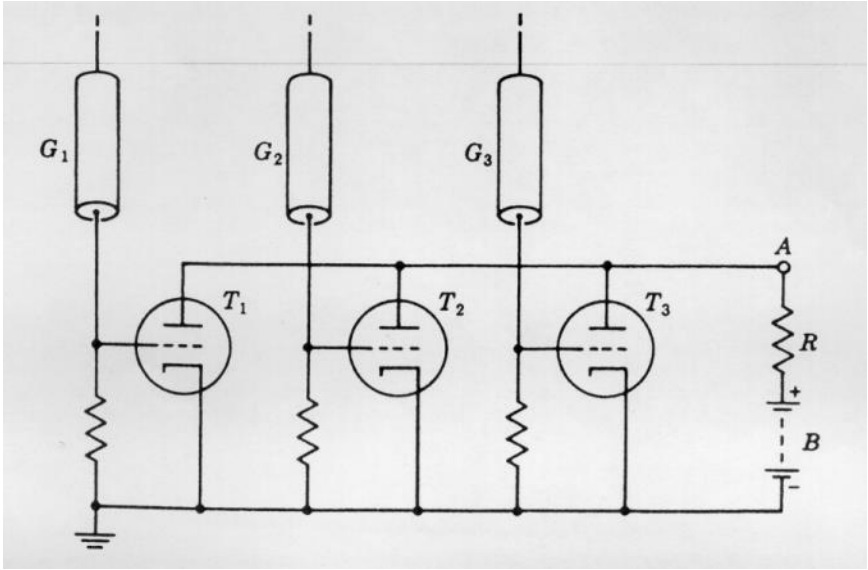

Cosmic ray telescope 1934

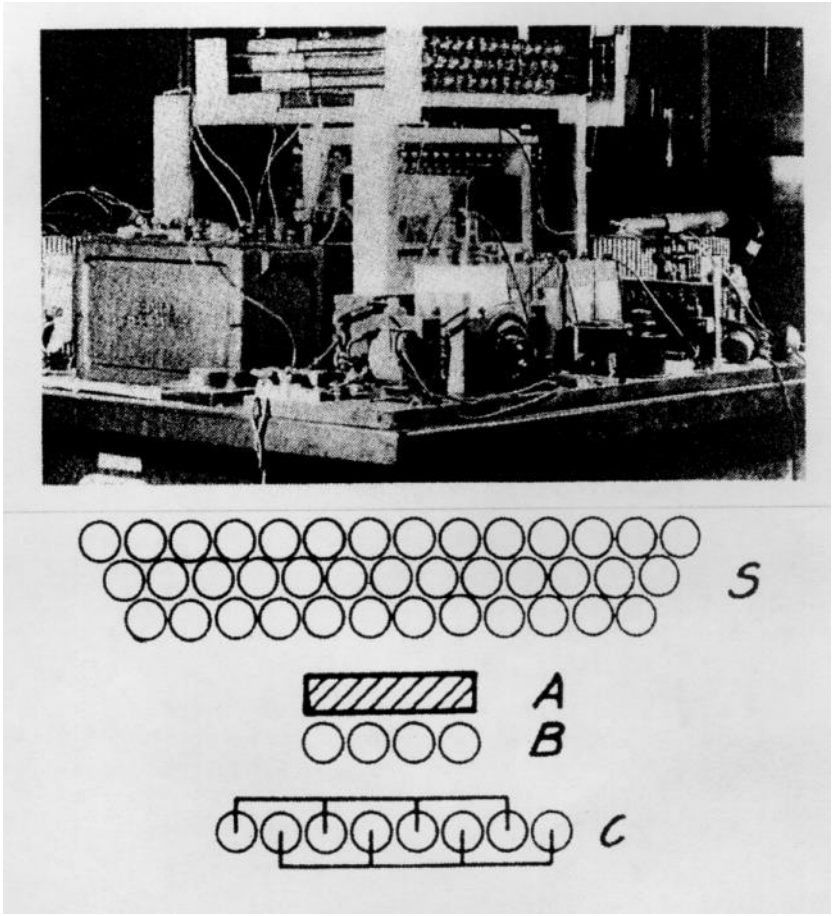

Geiger mode, large deadtime

Position resolution is determined by the size of the tubes.

Signal was directly fed into an electronic tube.

Multi Wire Proportional Chamber

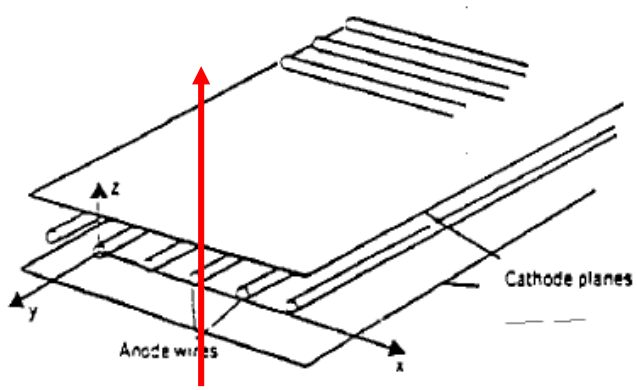

Abbildung 2.27: *Vieldrahtproportionalkammer.*

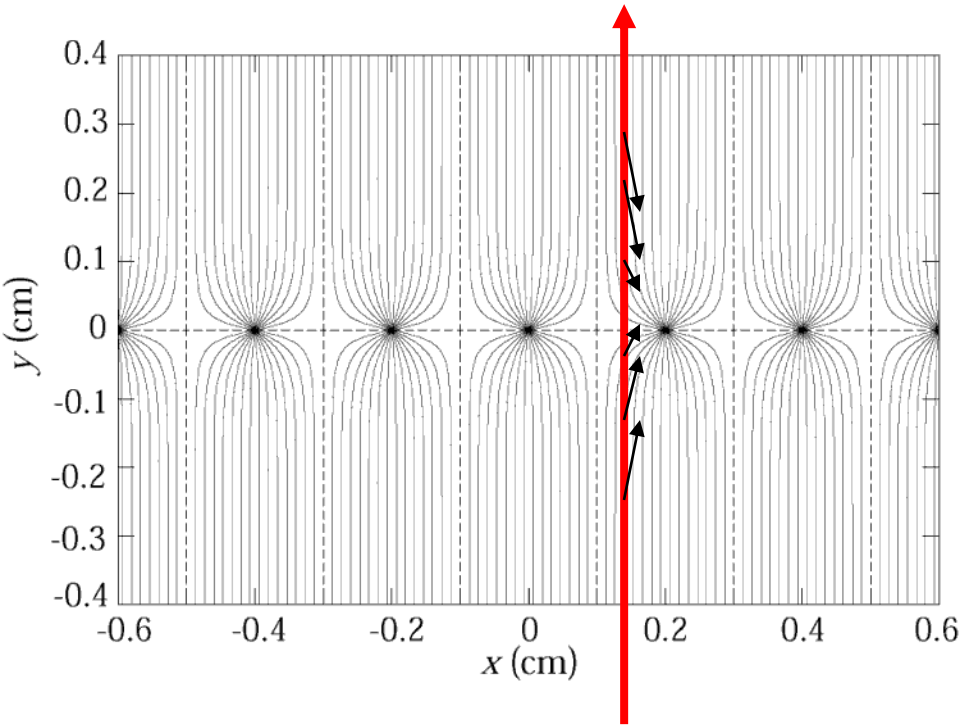

Classic geometry (Crossection), Charpak 1968 :

One plane of thin sense wires is placed between two parallel plates.

Typical dimensions:

Wire distance 2-5mm, distance between cathode planes ~10mm.

Electrons (v≈5cm/μs) are collected within ≈ 100ns. The ion tail can be eliminated by electronics filters → pulses of <100ns length.

For 10% occupancy → every μs one pulse

→ 1MHz/wire rate capabiliy !

→ Compare to Bubble Chamber with 10 Hz !

Multi Wire Proportional Chamber

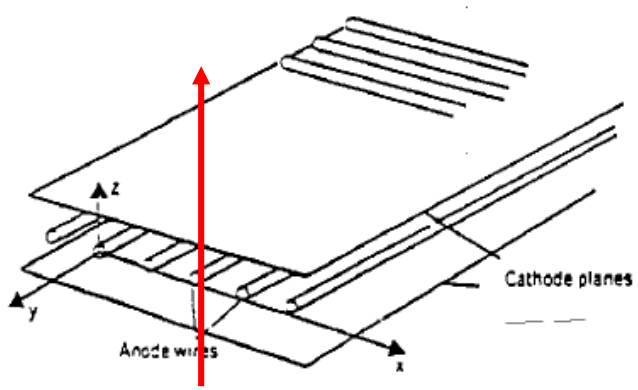

Abbildung 2.27: *Vieldrahtproportionalkammer.*

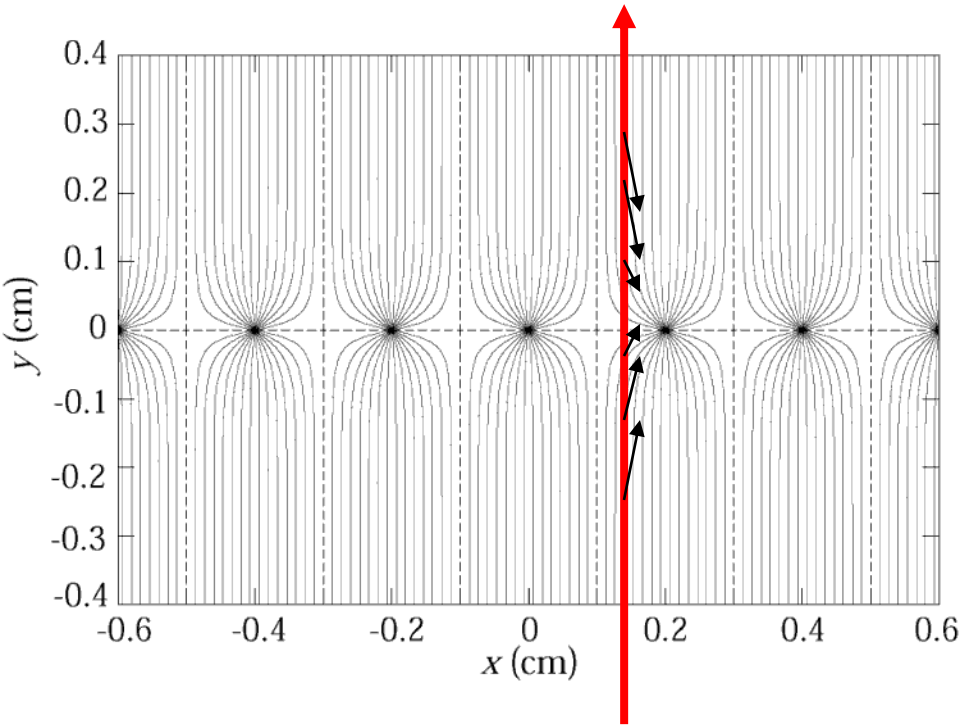

In order to eliminate the left/right ambiguities: Shift two wire chambers by half the wire pitch.

For second coordinate:

→Another chamber at 90^0 relative rotation

→Signal propagation to the two ends of the wire.

→Pulse height measurement on both ends of the wire. Because of resisitvity of the wire, both ends see different charge.

Segmenting of the cathode into strips or pads:

The movement of the charges induces a signal on the wire AND on the cathode. By segmentation of the cathode plane and charge interpolation, resolutions of 50μm can be achieved.

Multi Wire Proportional Chamber

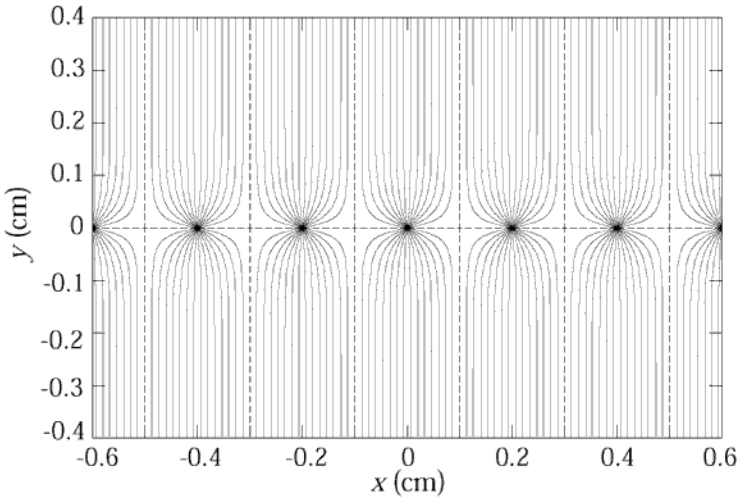

Cathode strip:

Width (1σ) of the charge distribution ≈ distance between Wires and cathode plane.

'Center of gravity' defines the particle trajectory.

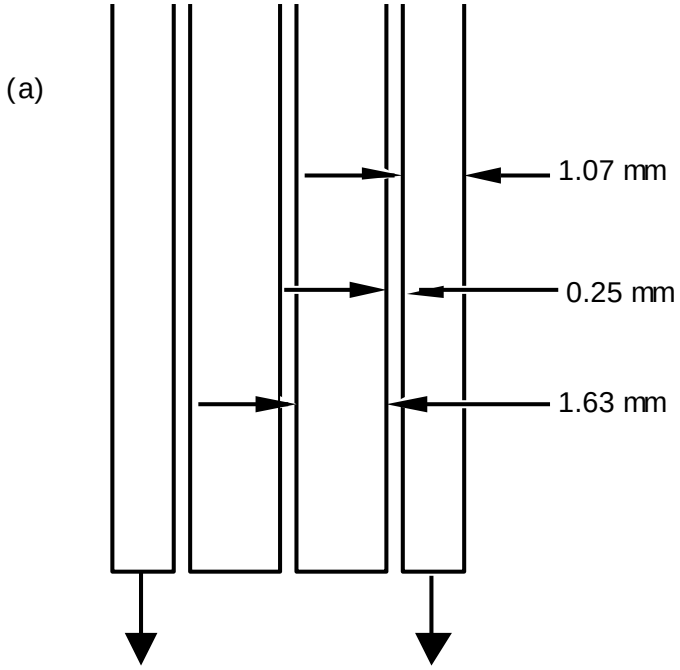

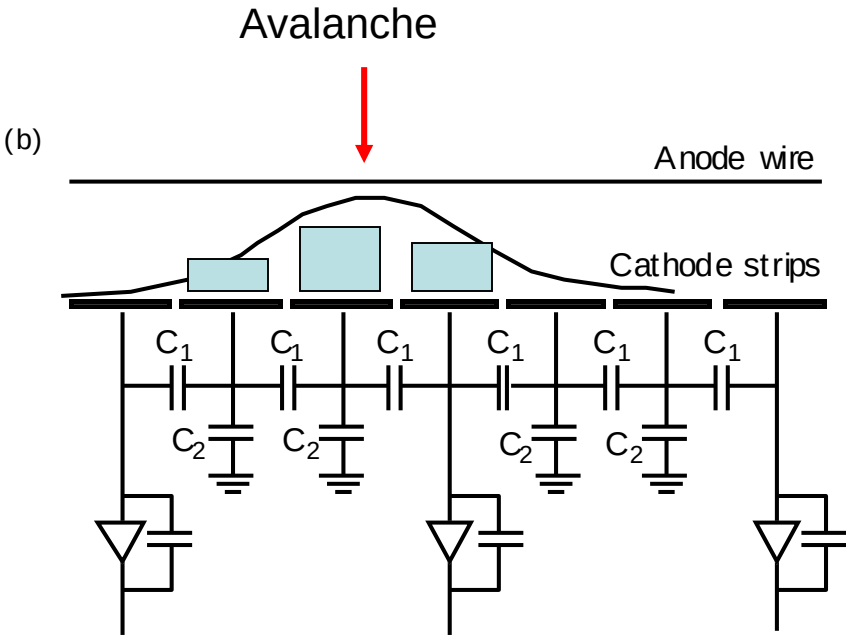

Drift Chambers

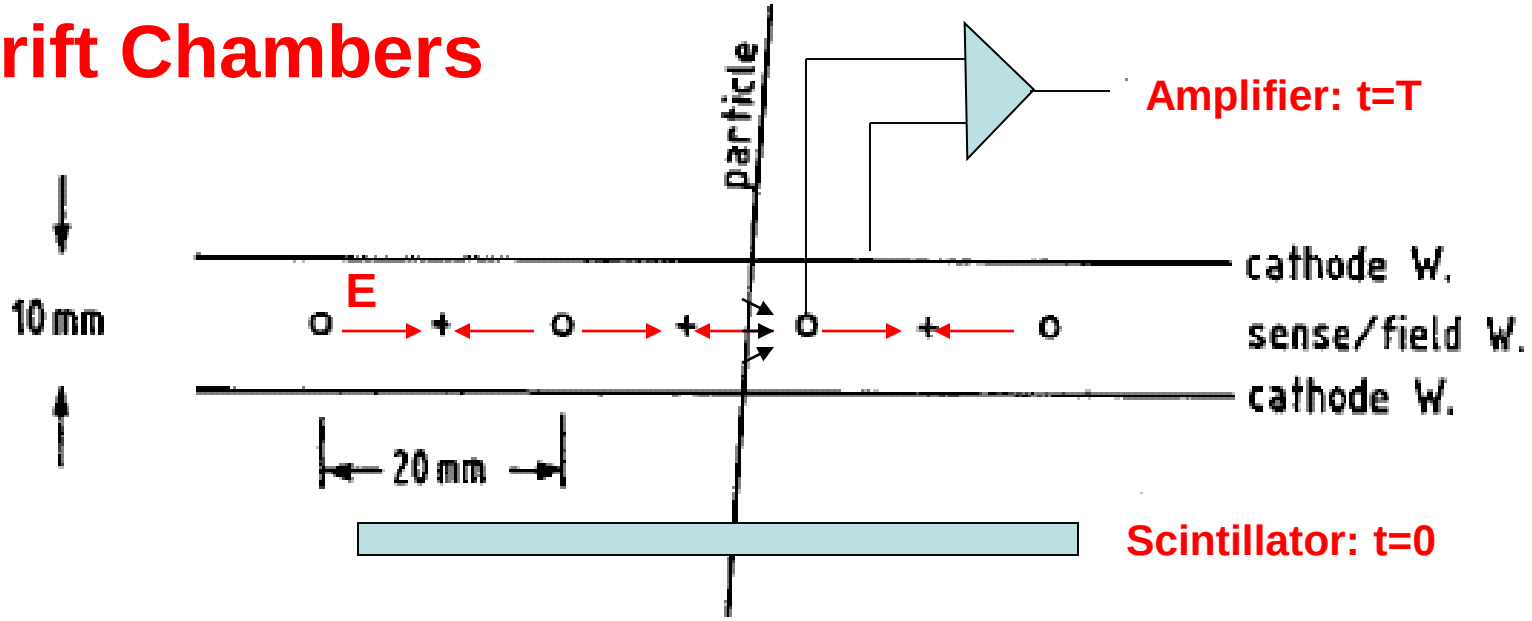

In an alternating sequence of wires with different potentials one finds an electric field between the 'sense wires' and 'field wires'.

The electrons are moving to the sense wires and produce an avalanche which induces a signal that is read out by electronics.

The time between the passage of the particle and the arrival of the electrons at the wire is measured.

The drift time T is a measure of the position of the particle !

By measuring the drift time, the wire distance can be increased (compared to the Multi Wire Proportional Chamber) → save electronics channels !

Drift Chambers, typical Geometries

Electric Field ≈ 1kV/cm

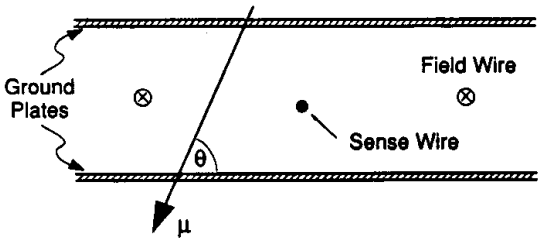

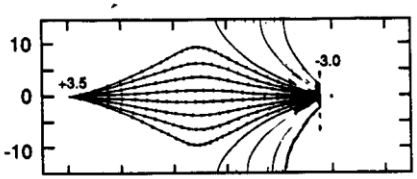

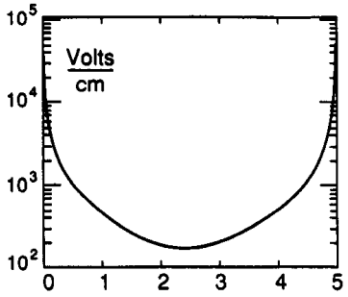

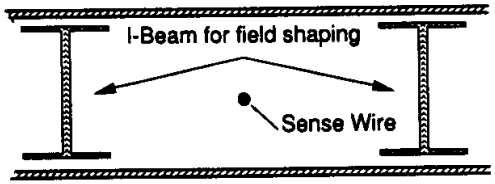

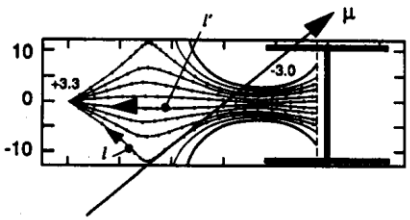

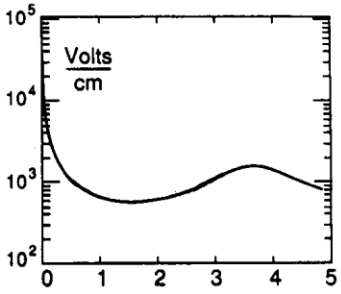

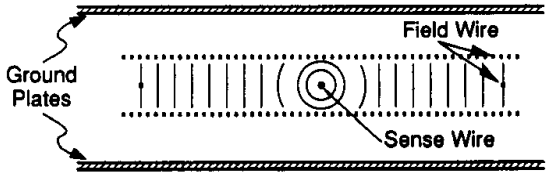

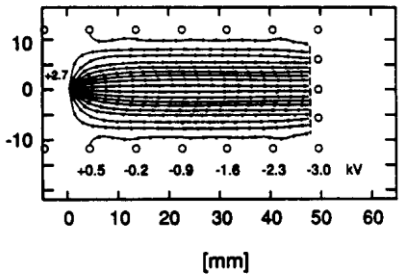

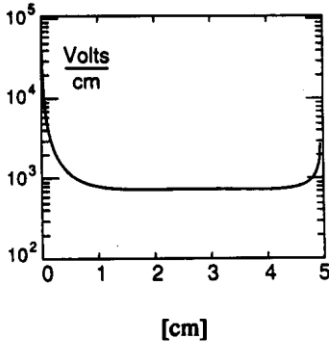

U.Becker Instr. of HEP, Vol#9, p516 World Scientific (1992) ed F.Sauli

The Geiger Counter reloaded: Drift Tube

ATLAS MDT R(tube) =15mm

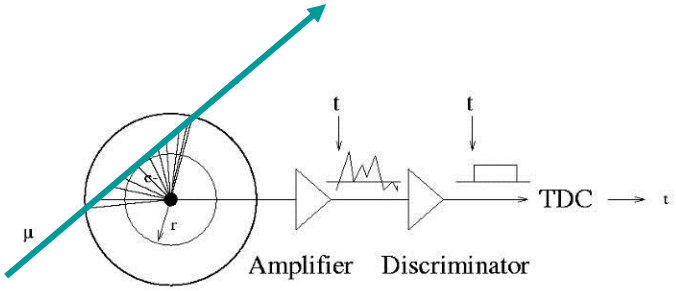

Calibrated Radius-Time correlation

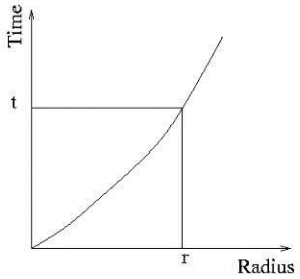

Primary electrons are drifting to the wire.

Electron avalanche at the wire.

The measured drift time is converted to a radius by a (calibrated) radius-time correlation.

Many of these circles define the particle track.

ATLAS Muon Chambers

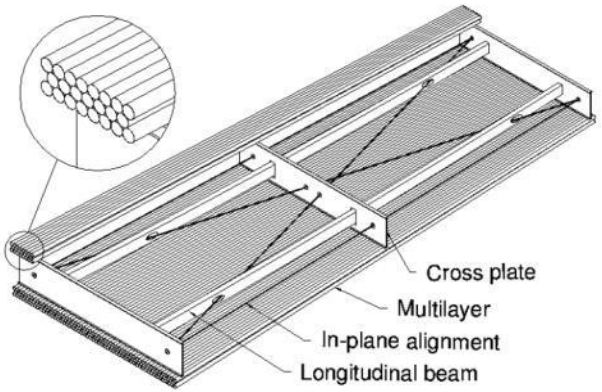

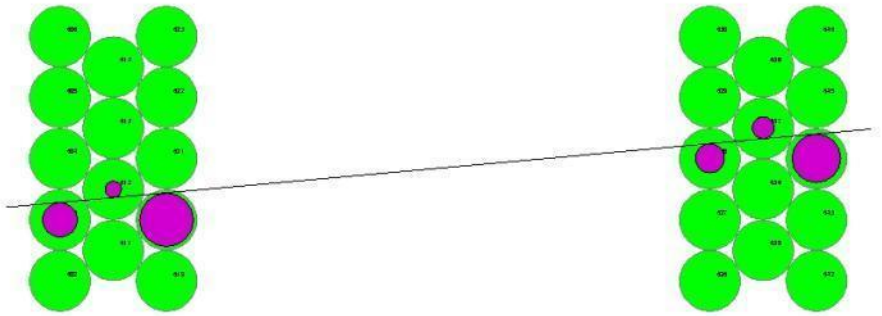

ATLAS MDTs, 80μm per tube

The Geiger counter reloaded: Drift Tube

Atlas Muon Spectrometer, 44m long, from r=5 to11m.

1200 Chambers

6 layers of 3cm tubes per chamber.

Length of the chambers 1-6m !

Position resolution: 80μm/tube, <50μm/chamber (3 bar)

Maximum drift time ≈700ns

Gas Ar/CO_2 93/7

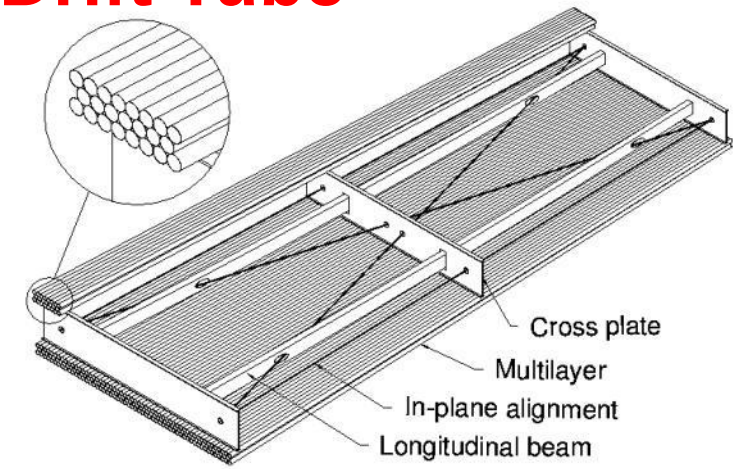

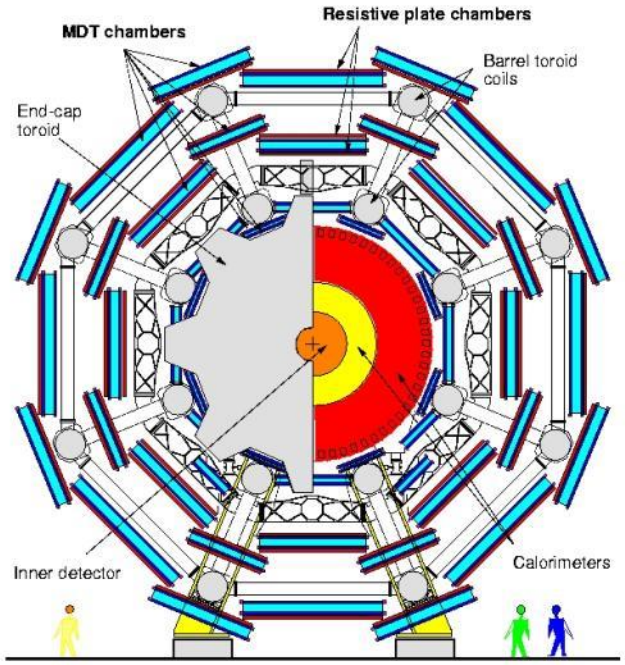

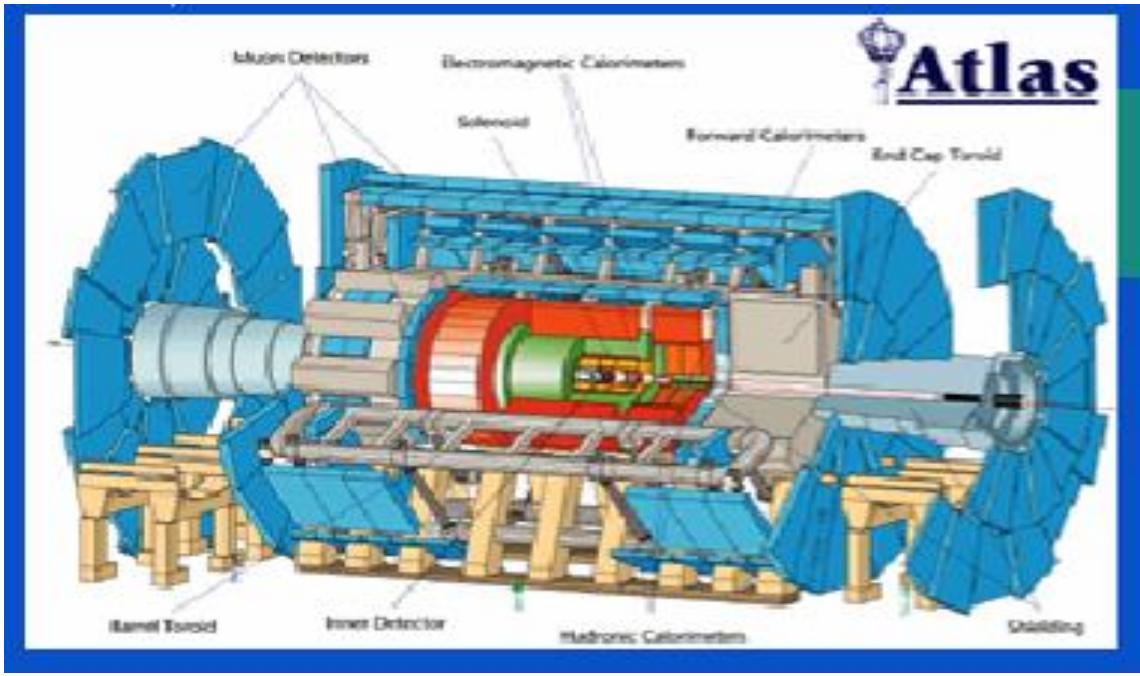

Large Drift Chambers

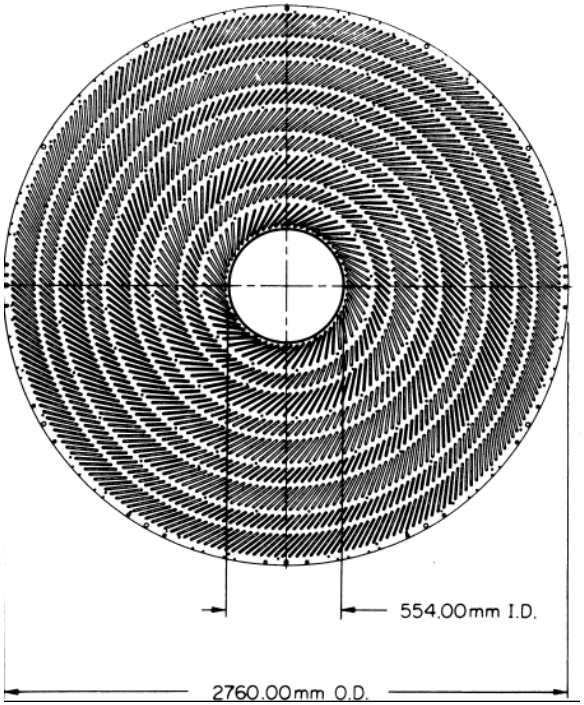

Central Tracking Chamber CDF Experiment.

660 drift cells tilted 45^0 with respect to the particle track.

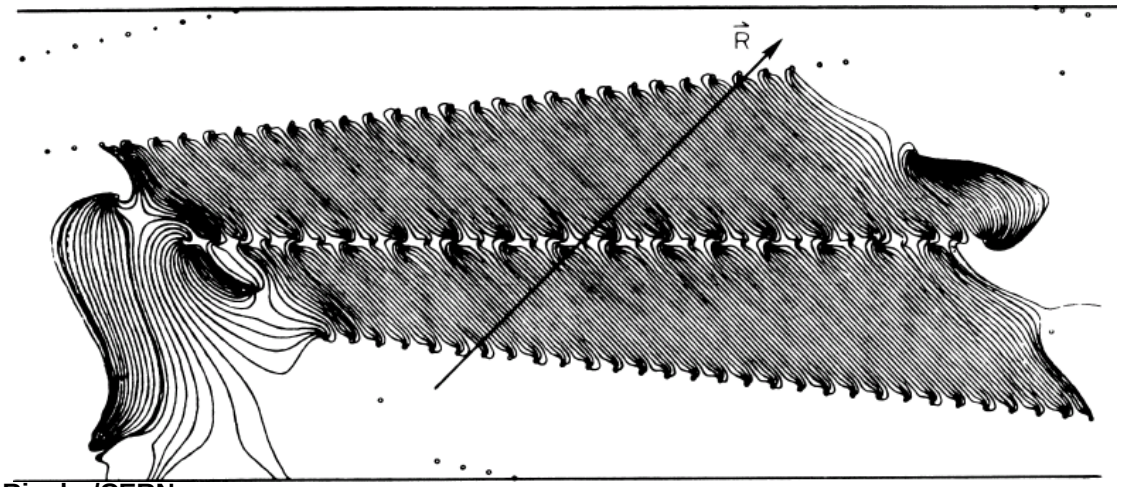

Drift cell

Time Projection Chamber (TPC):

Gas volume with parallel E and B Field.
B for momentum measurement. Positive effect:
Diffusion is strongly reduced by E//B (up to a factor 5).

Drift Fields 100-400V/cm. Drift times 10-100 μs.
Distance up to 2.5m !

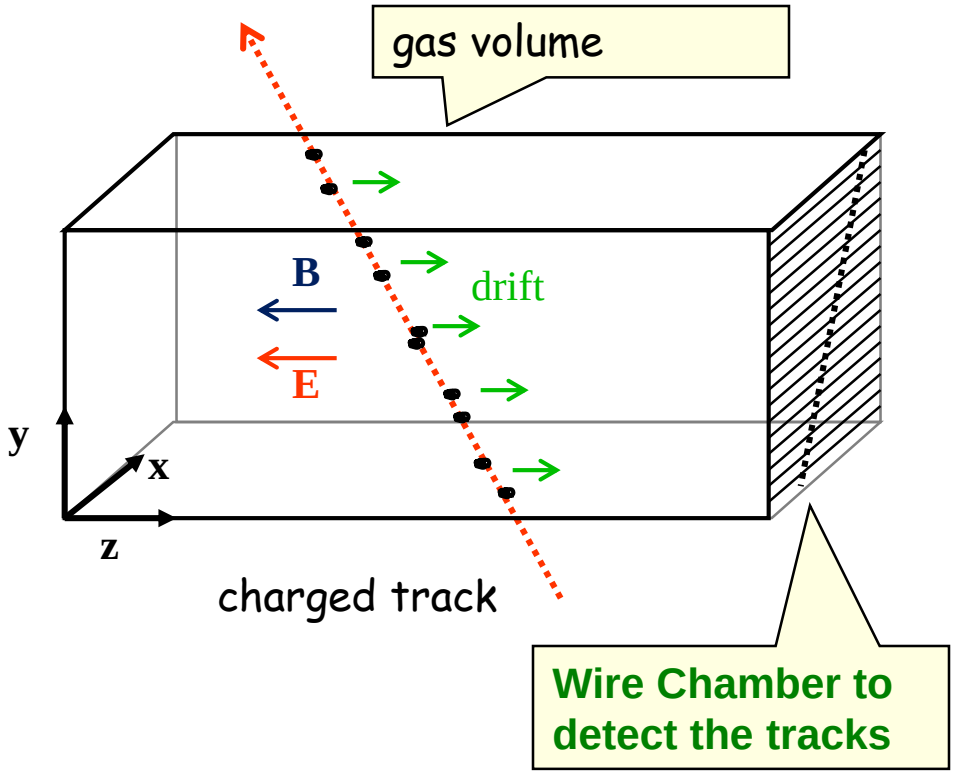

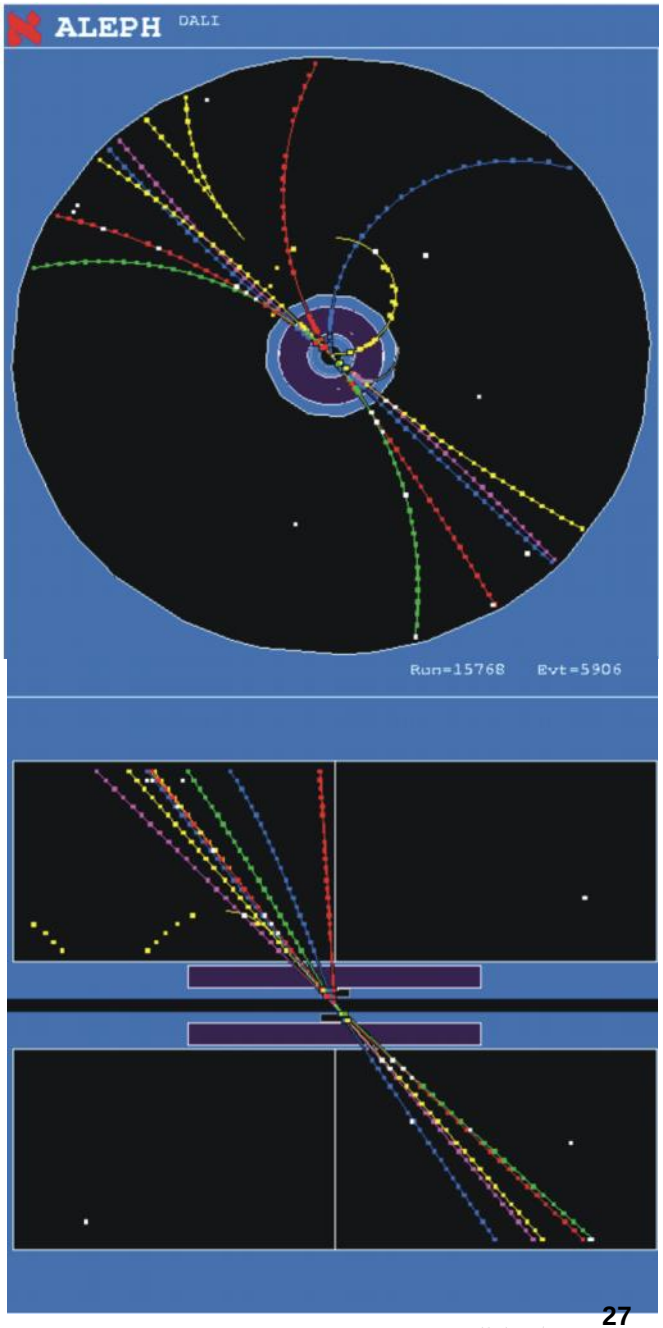

STAR TPC (BNL)

Event display of a Au Au collision at CM energy of 130 GeV/n.

Typically around 200 tracks per event.

Great advantage of a TPC: The only material that is in the way of the particles is gas → very low multiple scattering → very good momentum resolution down to low momenta !

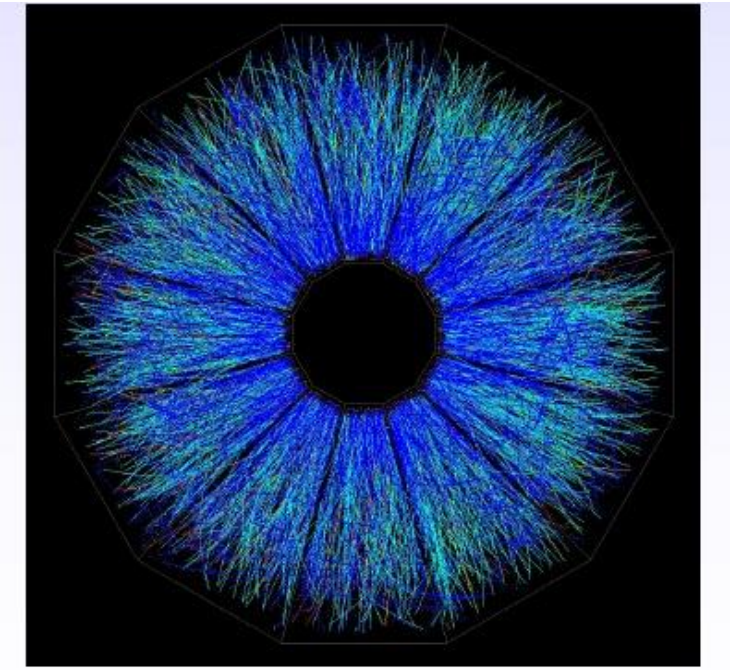

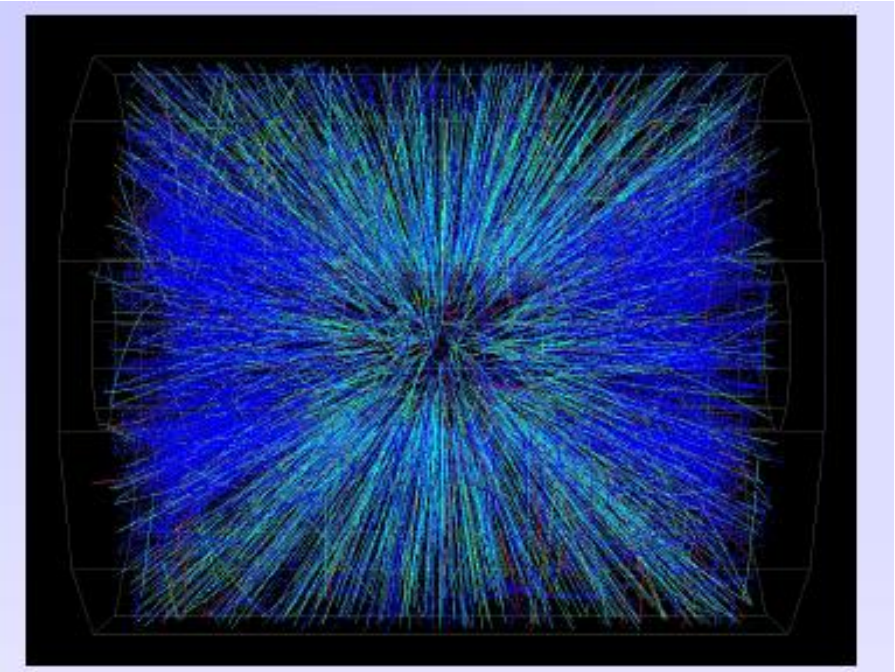

ALICE TPC: Detector Parameters

- Gas Ne/ CO_2 90/10%
- Field 400V/cm
- Gas gain >10^4
- Position resolution σ= 0.25mm
- Diffusion: σ_t= 250μm $\sqrt{cm}$
- Pads inside: 4x7.5mm
- Pads outside: 6x15mm
- B-field: 0.5T

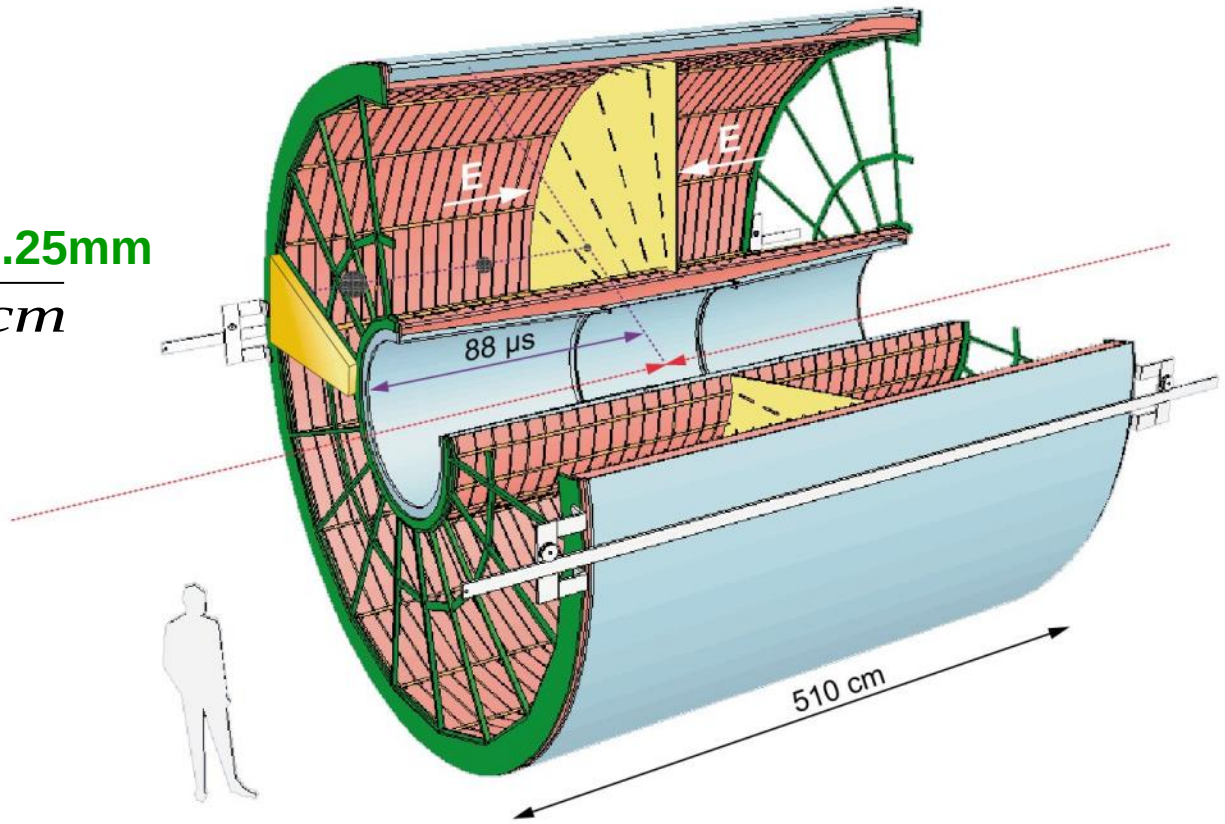

ALICE TPC: Construction Parameters

- **Largest TPC:**
  - **Length 5m**
  - **Diameter 5m**
  - **Volume 88m^3**
  - **Detector area 32m^2**
  - **Channels ~570 000**
- **High Voltage:**
  - **Cathode -100kV**
- **Material X_0**
  - **Cylinder from composite materials from airplane industry (X_0= ~3%)**

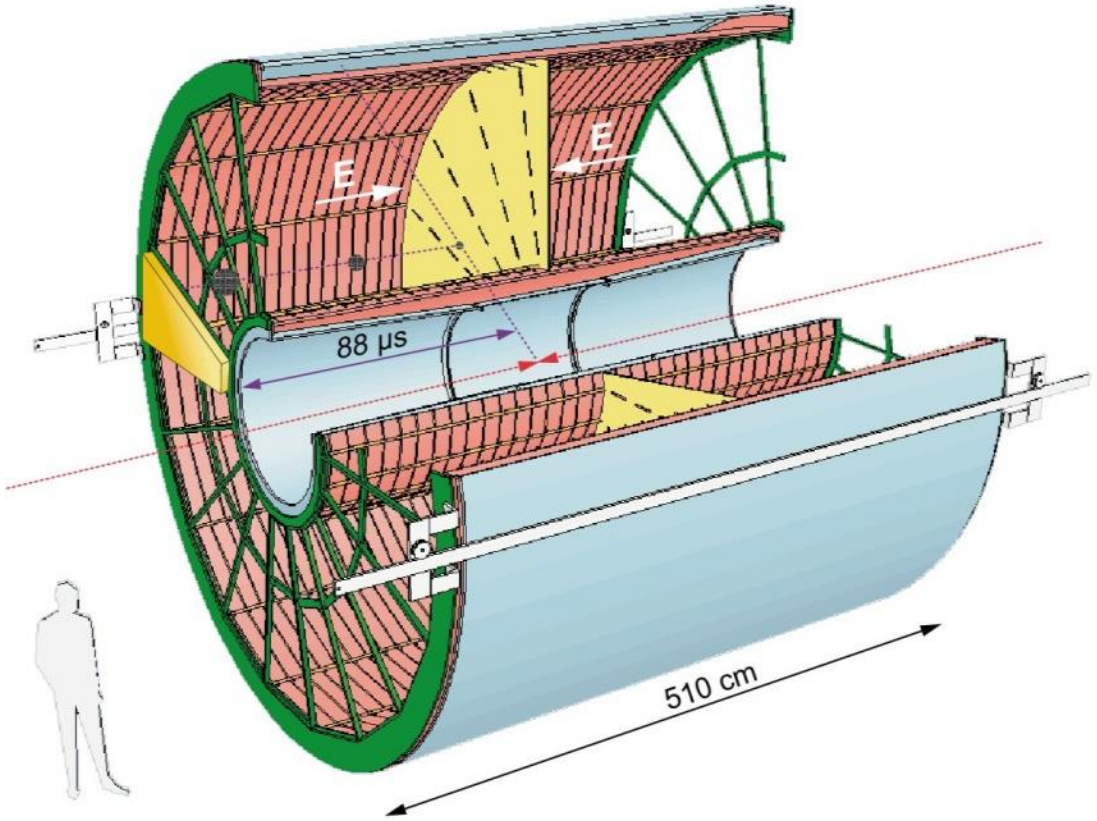

ALICE TPC: Pictures of the Construction

Precision in z: 250μm

End plates 250μm

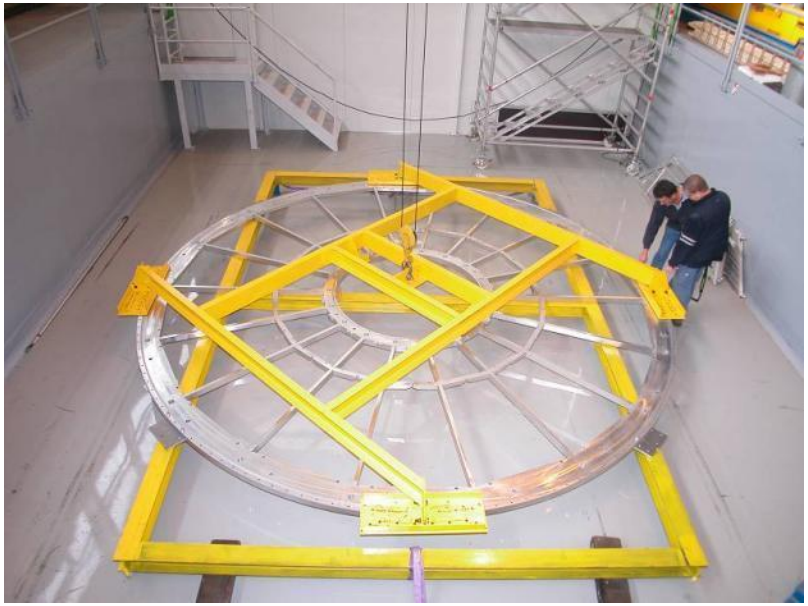

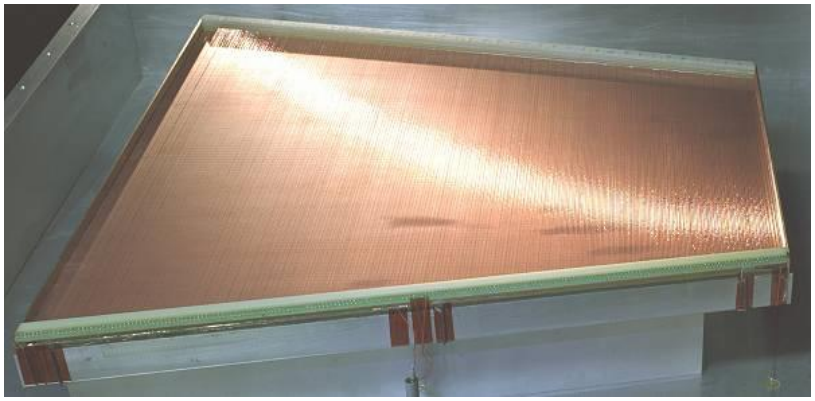

Wire chamber: 40μm

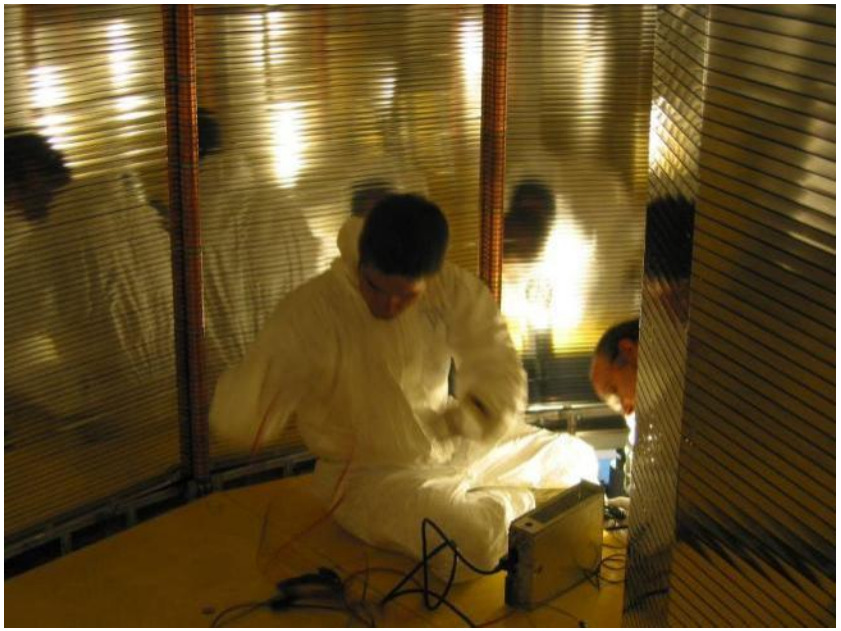

ALICE TPC Construction

My personal contribution:

A visit inside the TPC.

TPC installed in the ALICE Experiment

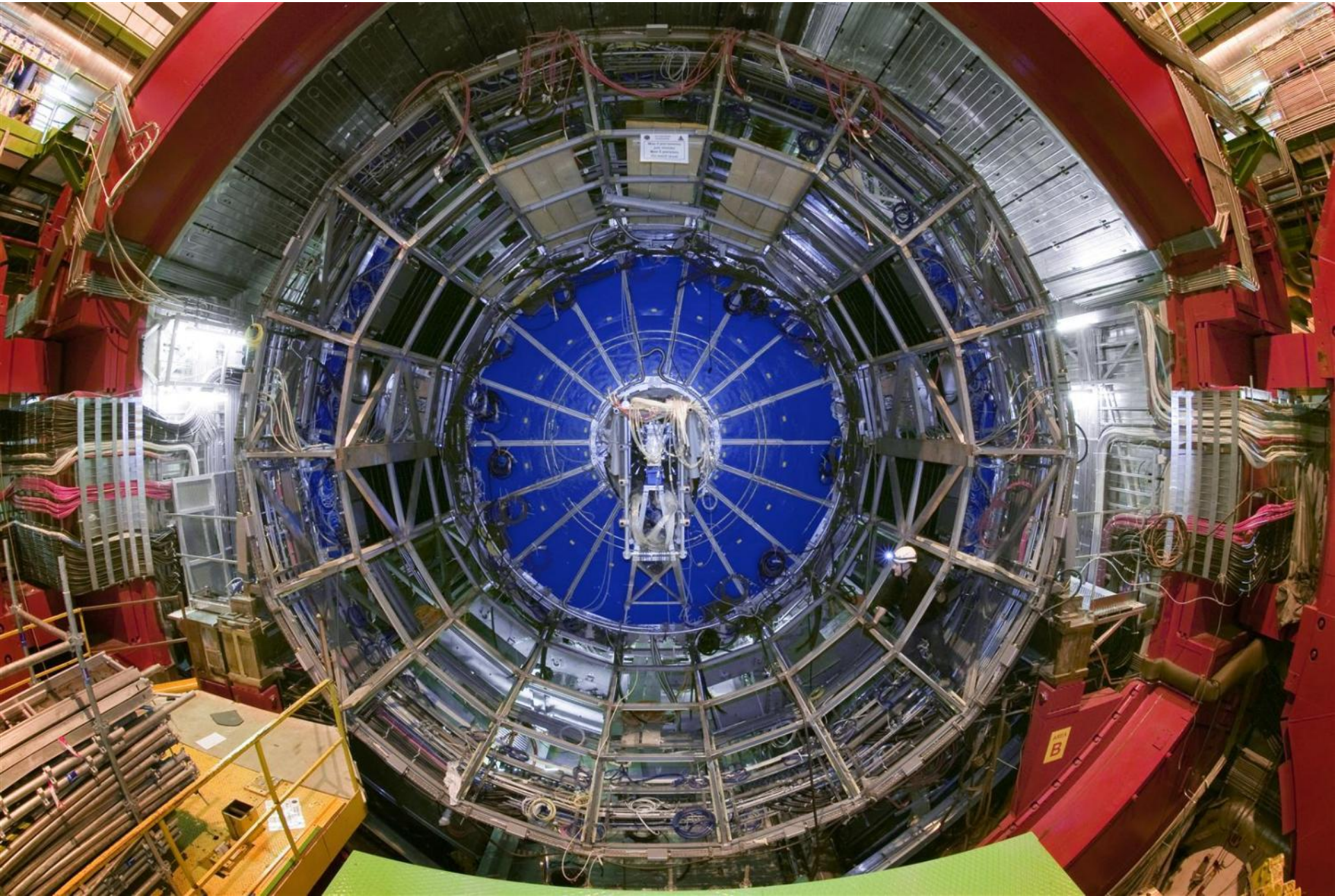

First 7 TeV p-p Collisions in the ALICE TPC in March 2010 !

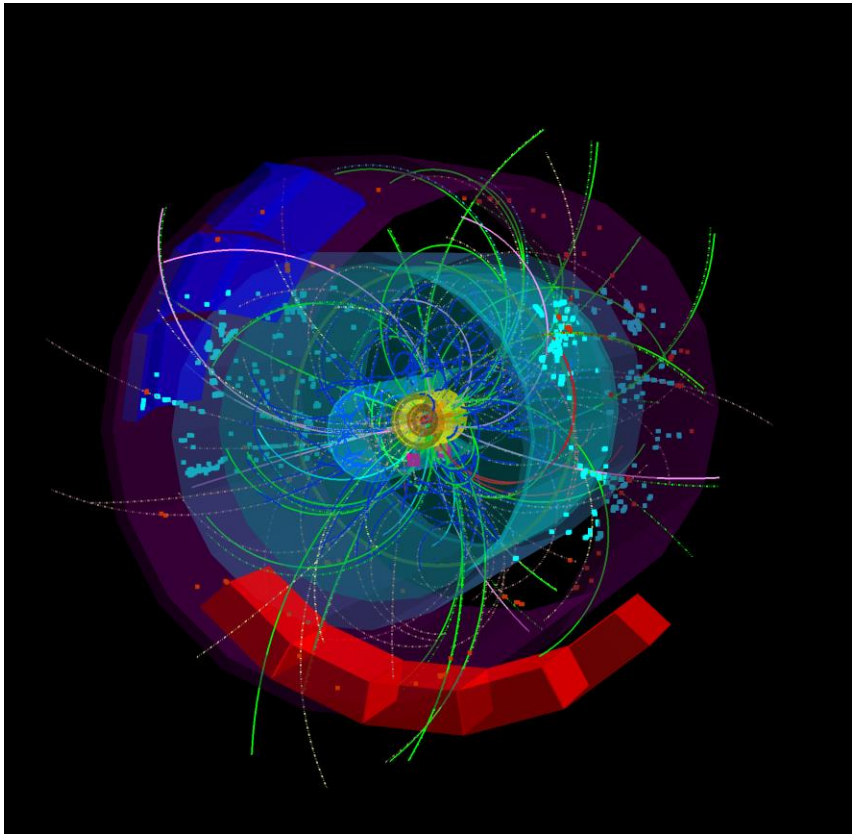

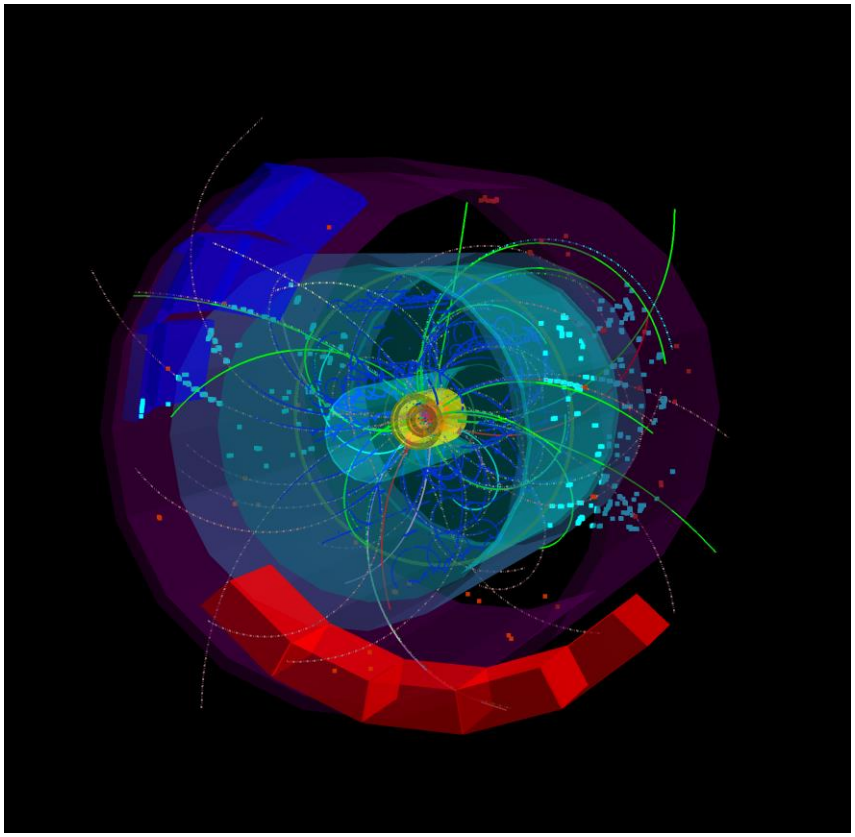

First Pb Pb Collisions in the ALICE TPC in Nov 2010 !

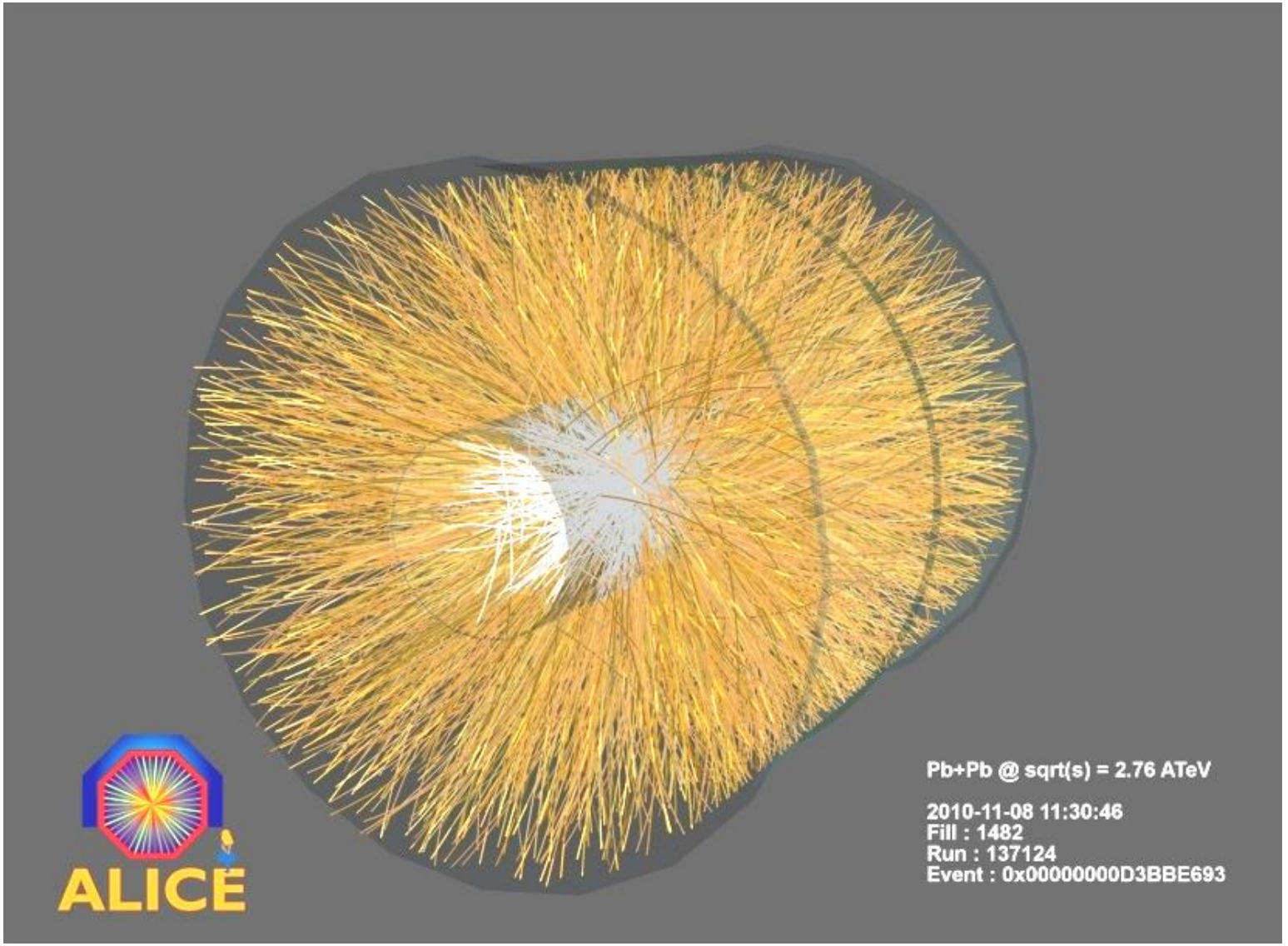

GEMs & MICROMEGAS

MICROMEGAS

Narrow gap (50-100 μm) PPC with thin cathode mesh
Insulating gap-restoring wires or pillars

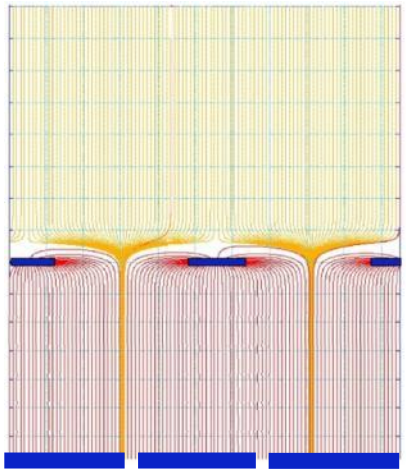

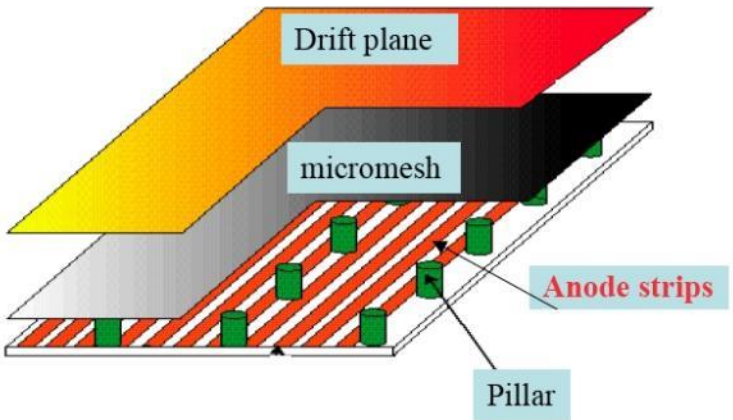

Y. Giomataris et al, Nucl. Instr. and Meth. A376(1996)239

GEM

Thin metal-coated polymer foils
70 μm holes at 140 mm pitch

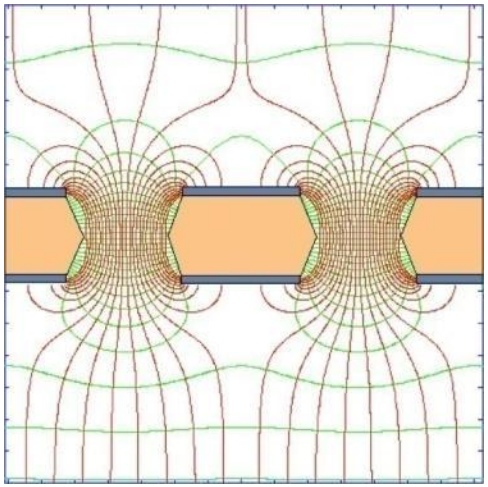

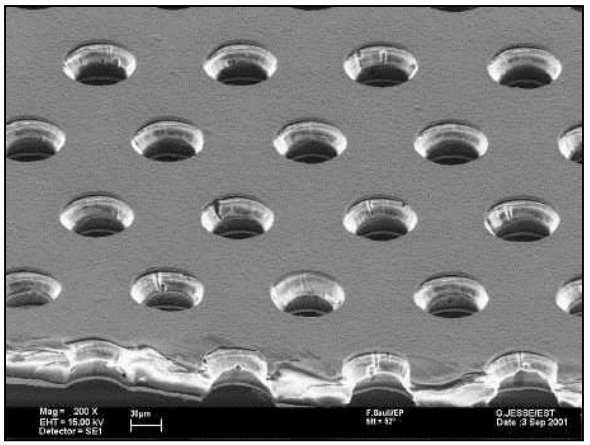

F. Sauli, Nucl. Instr. and Methods A386(1997)531

Summary on Gas Detectors

Wire chambers feature prominently at LHC. A decade of very extensive studies on gases and construction materials has lead to wire chambers that can track up to MHz/cm^2 of particles, accumulate up to 1-2C/cm of wire and 1-2 C/cm^2 of cathode area.

While silicon trackers currently outperform wire chambers close to the interaction regions, wire chambers are perfectly suited for the large detector areas at outer radii.

Large scale next generation experiments foresee wire chambers as large area tracking devices.

The Time Projection Chamber – if the rate allows it's use – is unbeatable in terms of low material budget and channel economy. There is no reason for replacing a TPC with a silicon tracker.

Gas detectors can be simulated very accurately due to excellent simulation programs.

Novel gas detectors, the Micro Pattern Gas Detectors, have proven to work efficiently as high rate, low material budget trackers in the 'regime' between silicon trackers and large wire chambers.

Solid State Detectors

Gas Detectors

In gaseous detectors, a charged particle is liberating electrons from the atoms, which are freely bouncing between the gas atoms.

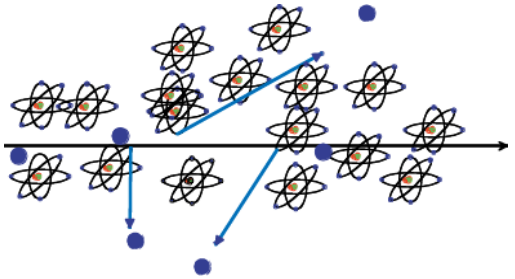

An applied electric field makes the electrons and ions move, which induces signals on the metal readout electrodes.

For individual gas atoms, the electron energy levels are discrete.

Solid State Detectors

In solids (crystals), the electron energy levels are in ‘bands’.

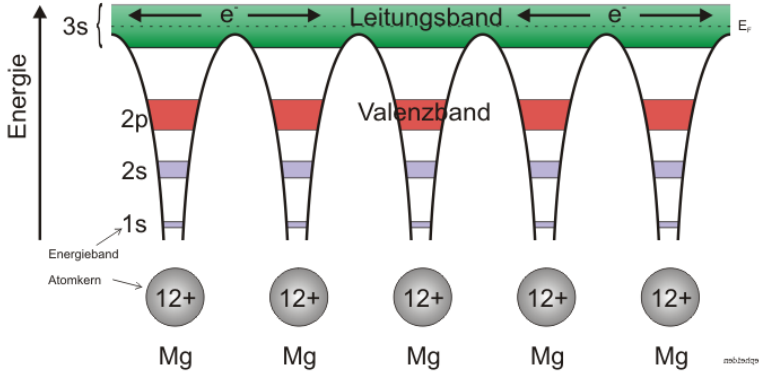

Inner shell electrons, in the lower energy bands, are closely bound to the individual atoms and always stay with ‘their’ atoms.

In a crystal there are however energy bands that are still bound states of the crystal, but they belong to the entire crystal. Electrons in these bands and the holes in the lower band can freely move around the crystal, if an electric field is applied.

Solid State Detectors

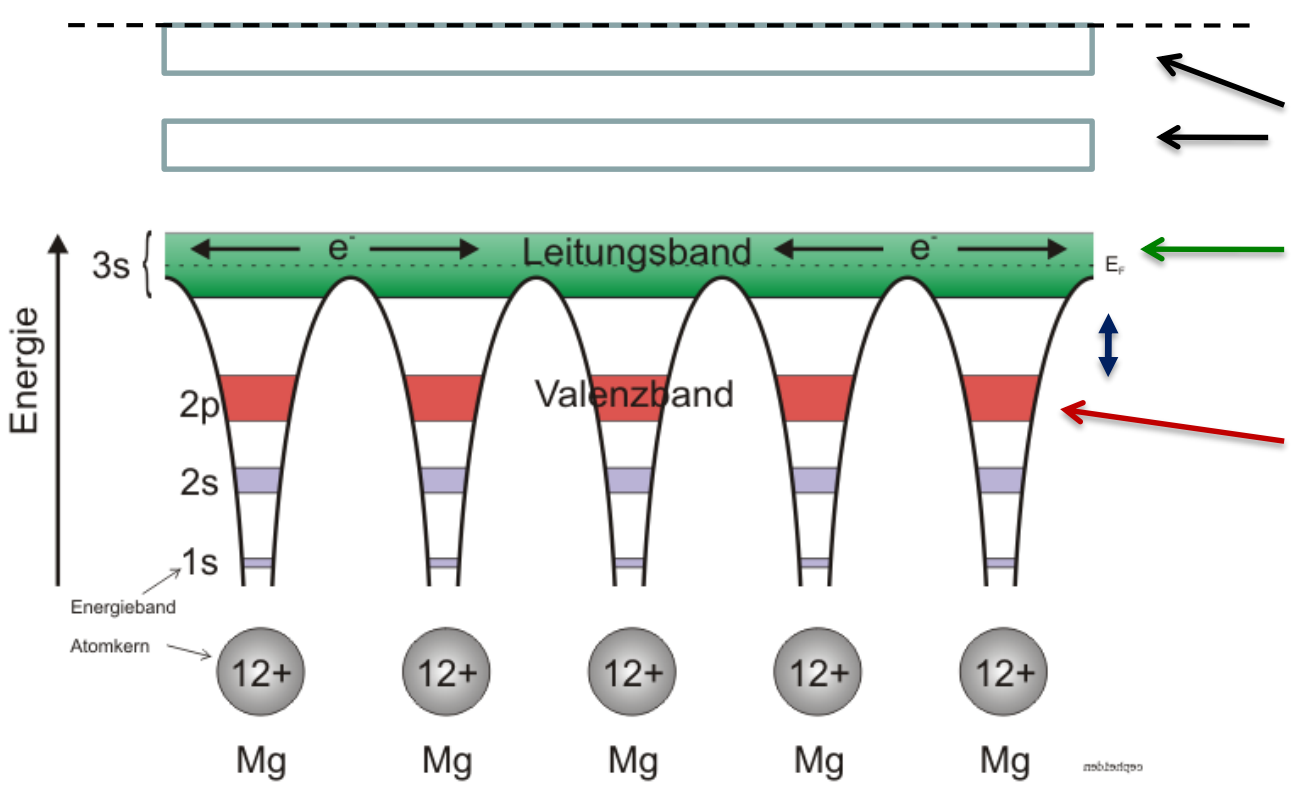

Conductor, Insulator, Semiconductor

In case the conduction band is filled the crystal is a conductor.

In case the conduction band is empty and 'far away' from the valence band, the crystal is an insulator.

In case the conduction band is empty but the distance to the valence band is small, the crystal is a semiconductor.

Solid State Detectors

Band Gap, e-h pair Energy

The energy gap between the last filled band – the valence band – and the conduction band is called band gap E_g.

The band gap of Diamond/Silicon/Germanium is 5.5, 1.12, 0.66 eV.

The average energy to produce an electron/hole pair for Diamond/Silicon/Germanium is 13, 3.6, 2.9eV.

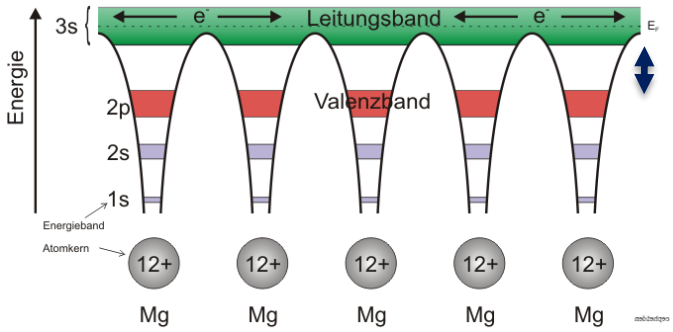

Temperature, Charged Particle Detection

In case an electron in the valence band gains energy by some process, it can be excited into the conduction band and a hole in the valence band is left behind.

Such a process can be the passage of a charged particle, but also thermal excitation → probability is proportional Exp(-E_g/kT).

The number of electrons in the conduction band is therefore increasing with temperature i.e. the conductivity of a semiconductor increases with temperature.

Solid State Detectors

Electron, Hole Movement:

It is possible to treat electrons in the conduction band and holes in the valence band similar to free particles, but with an effective mass different from elementary electrons not embedded in the lattice.

This mass is furthermore dependent on other parameters such as the direction of movement with respect to the crystal axis. All this follows from the QM treatment of the crystal (solid state physics).

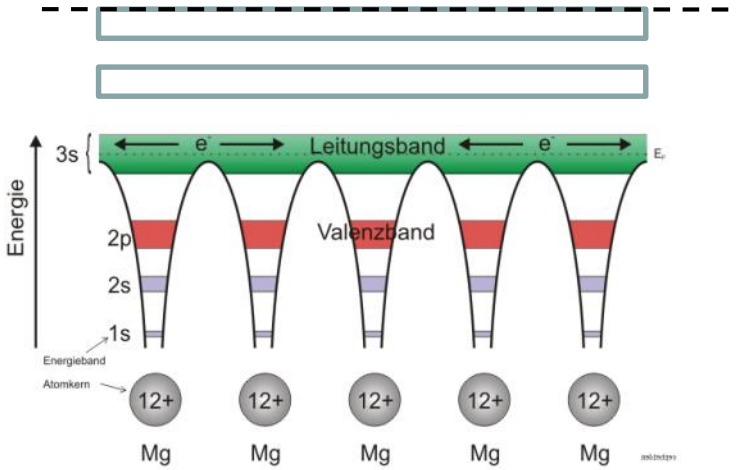

Cooling:

If we want to use a semiconductor as a detector for charged particles, the number of charge carriers in the conduction band due to thermal excitation must be smaller than the number of charge carriers in the conduction band produced by the passage of a charged particle.

Diamond (E_g=5.5eV) can be used for particle detection at room temperature,
Silicon (E_g=1.12 eV) and Germanium (E_g=0.66eV) must be cooled, or the free charge carriers must be eliminated by other tricks → doping → see later.

Solid State Detectors

Primary 'ionization':

The average energy to produce an electron/hole pair is: Diamond (13eV), Silicon (3.6eV), Germanium (2.9eV)

Comparing to gas detectors, the density of a solid is about a factor 1000 larger than that of a gas and the energy to produce and electron/hole pair e.g. for Si is a factor 7 smaller than the energy to produce an electron-ion pair in Argon.

Solid State vs. Gas Detector:

The number of primary charges in a Si detector is therefore about 10^4 times larger than the one in gas → while gas detectors need internal charge amplification, solid state detectors don't need internal amplification.

While in gaseous detectors, the velocity of electrons and ions differs by a factor 1000, the velocity of electrons and holes in many semiconductor detectors is quite similar → very short signals.

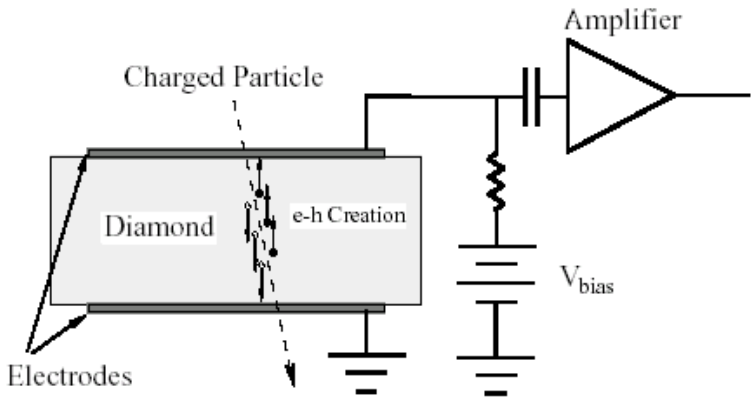

Diamond → A solid state ionization chamber

Diamond Detector

Typical thickness – a few 100μm.

<1000 charge carriers/cm^3 at room temperature due to large band gap.

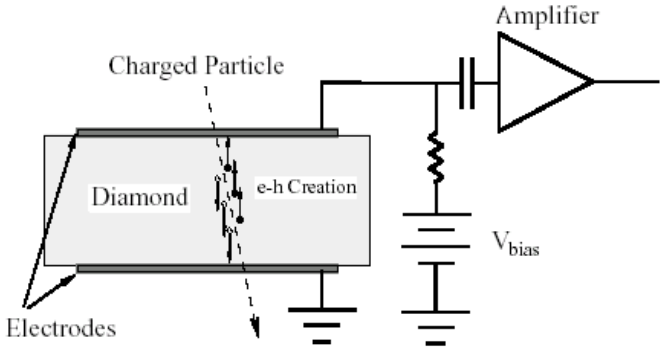

Velocity:

μ_e=1800 cm^2/Vs, μ_h=1600 cm^2/Vs

Velocity = μE, 10kV/cm → v=180 μm/ns → Very fast signals of only a few ns length !

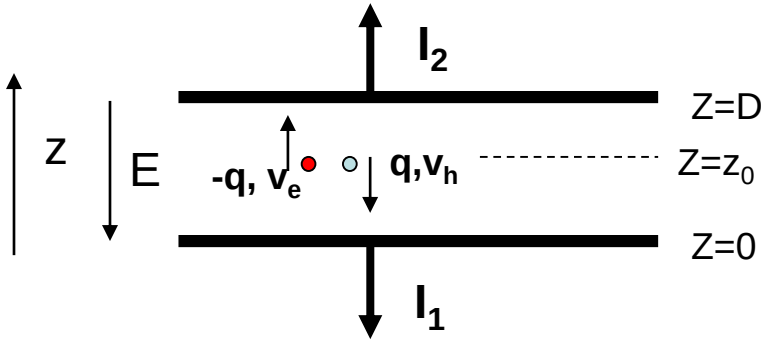

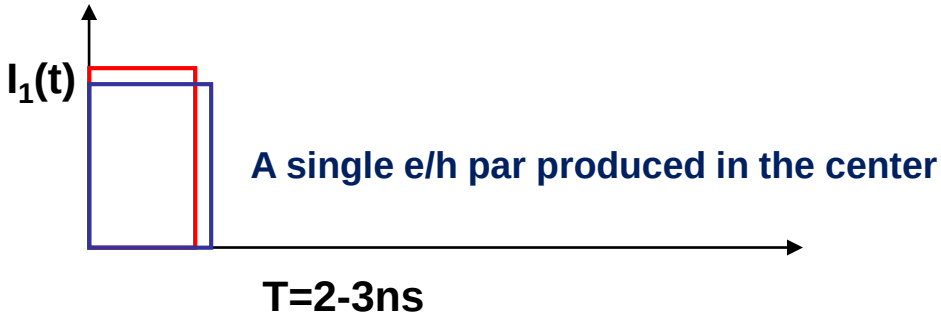

Diamond Detector

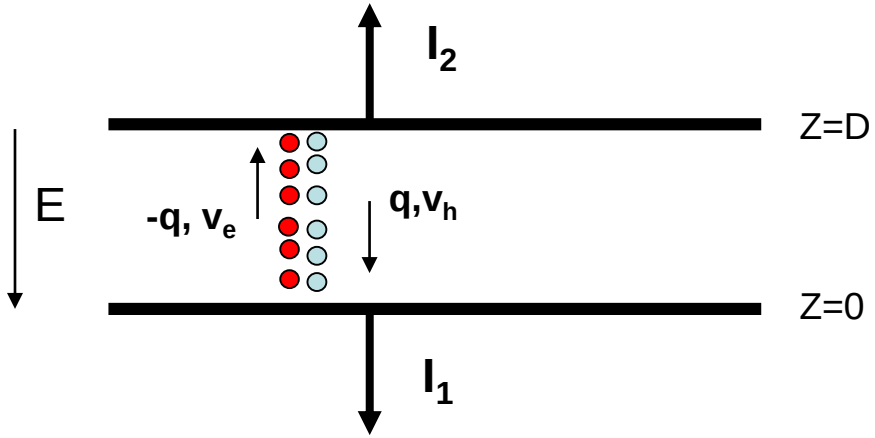

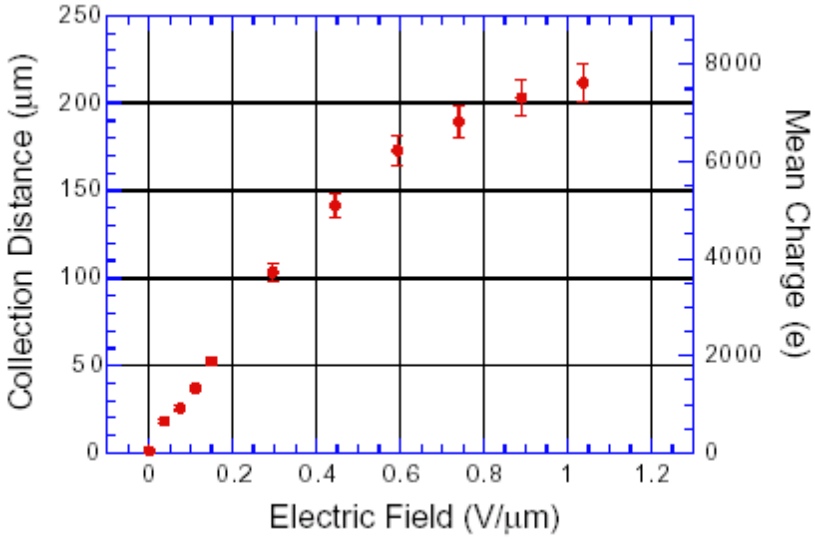

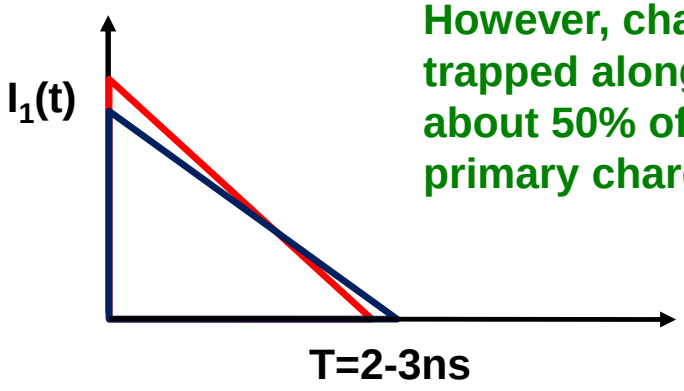

However, charges are trapped along the track, only about 50% of *produced* primary charge is *induced* →

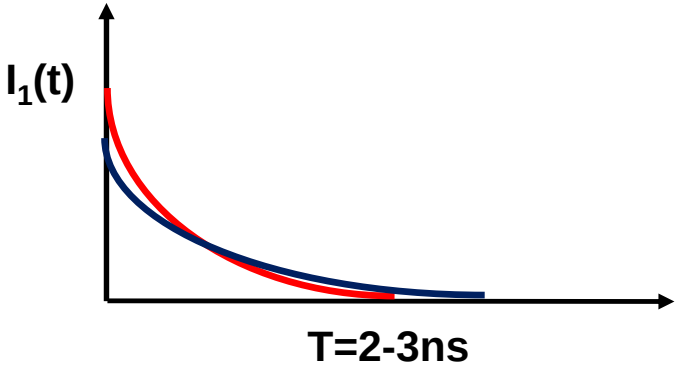

Silicon Detector

Velocity:
μ_e=1450 cm^2/Vs, μ_h=505 cm^2/Vs, 3.63eV per e-h pair.
~33000 e/h pairs in 300µm of silicon.

However: Free charge carriers in Si:
T=300 K: e,h = 1.45 x 10^{10} / cm^3 but only 33000 e/h pairs in 300µm produced by a high energy particle.

Why can we use Si as a solid state detector ???

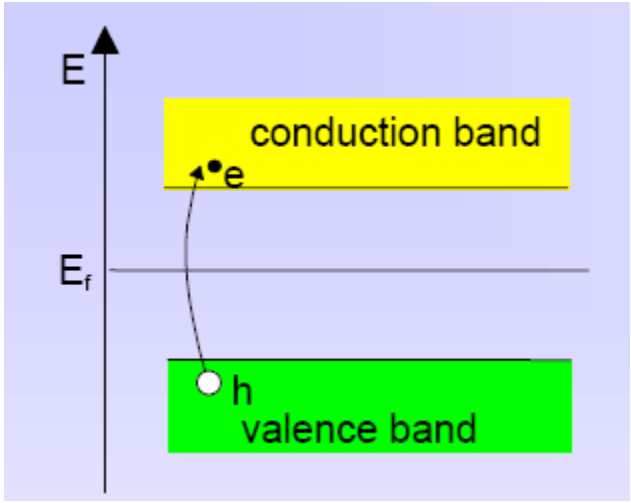

Doping of Silicon

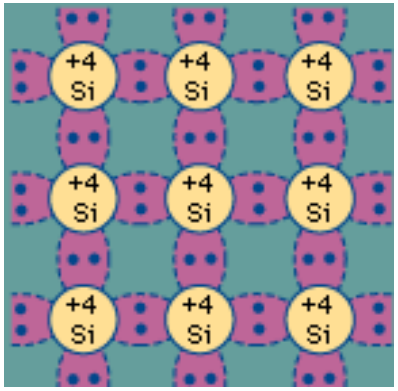

doping

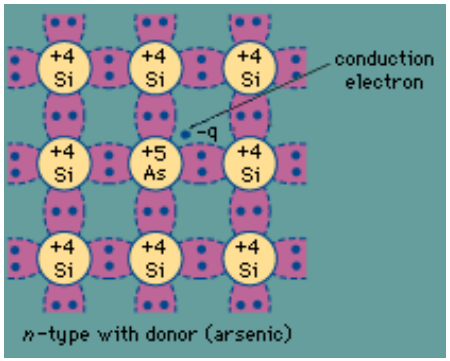

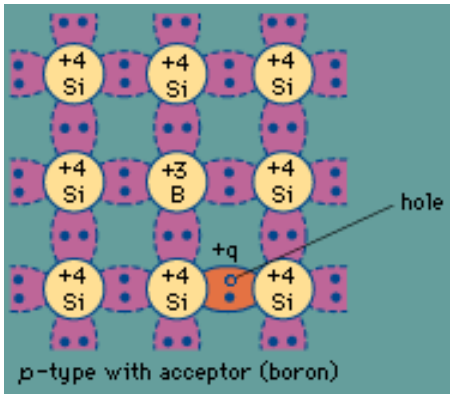

In a silicon crystal at a given temperature the number of electrons in the conduction band is equal to the number of holes in the valence band.

Doping Silicon with Arsen (+5) it becomes and n-type conductor (more electrons than holes).

Doping Silicon with Boron (+3) it becomes a p-type conductor (more holes than electrons).

Bringing p and n in contact makes a diode.

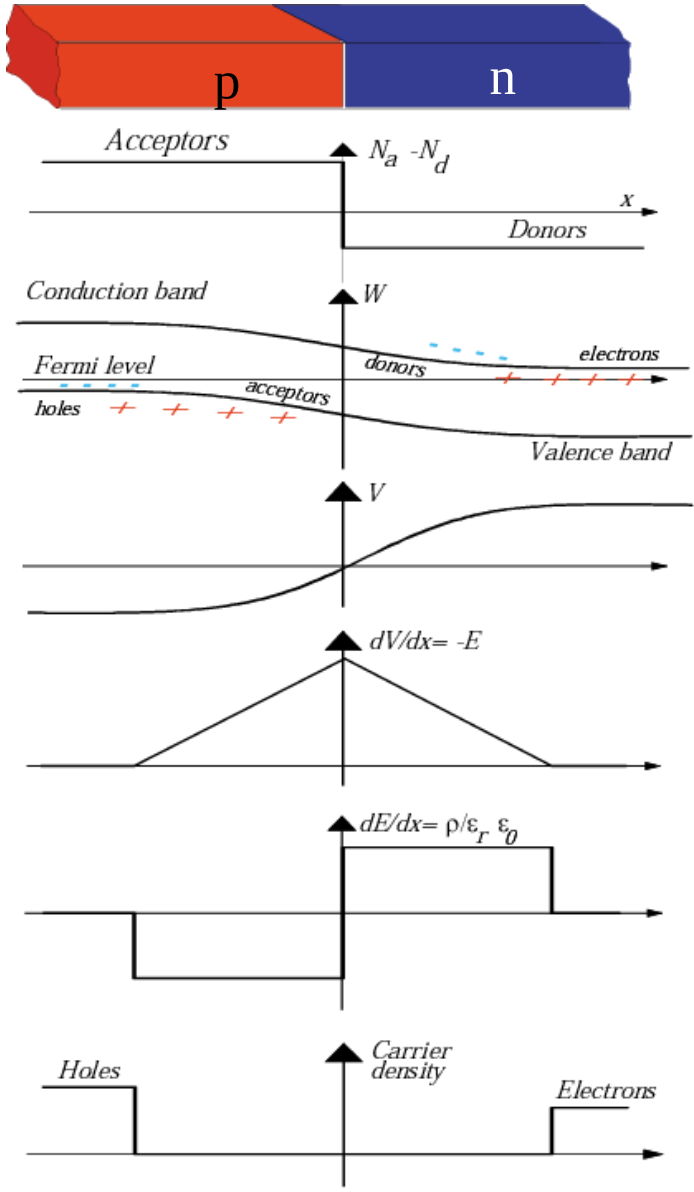

Si-Diode used as a Particle Detector !

At the p-n junction the charges are depleted and a zone free of charge carriers is established.

By applying a voltage, the depletion zone can be extended to the entire diode → highly insulating layer.

An ionizing particle produces free charge carriers in the diode, which drift in the electric field and induce an electrical signal on the metal electrodes.

As silicon is the most commonly used material in the electronics industry, it has one big advantage with respect to other materials, namely highly developed technology.

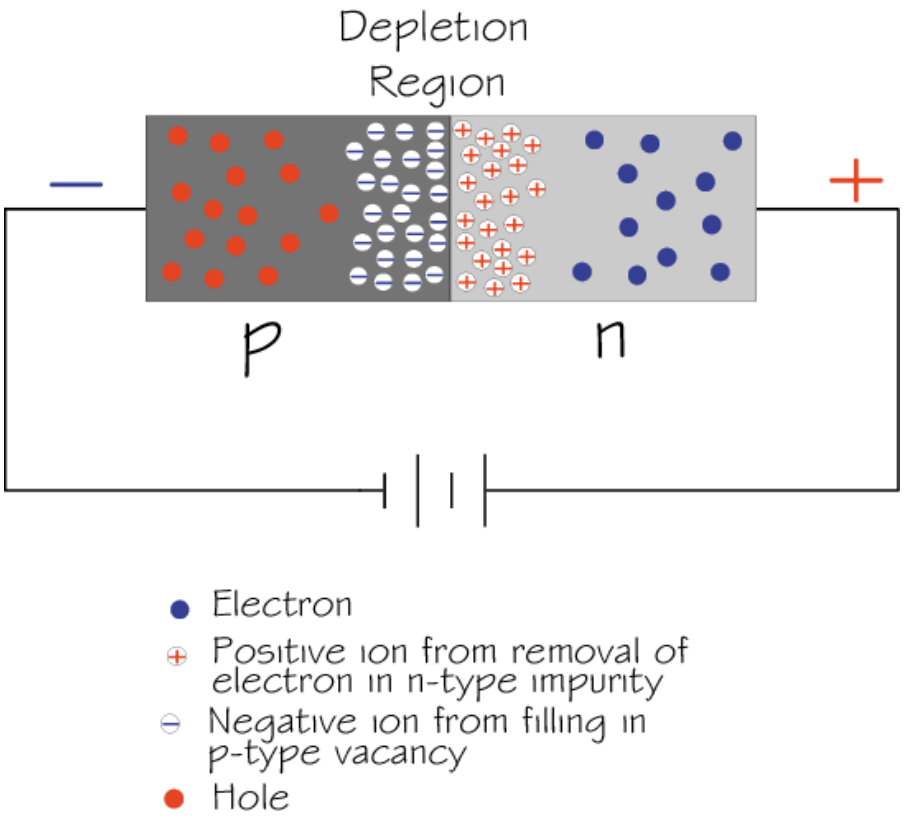

Under-Depleted Silicon Detector

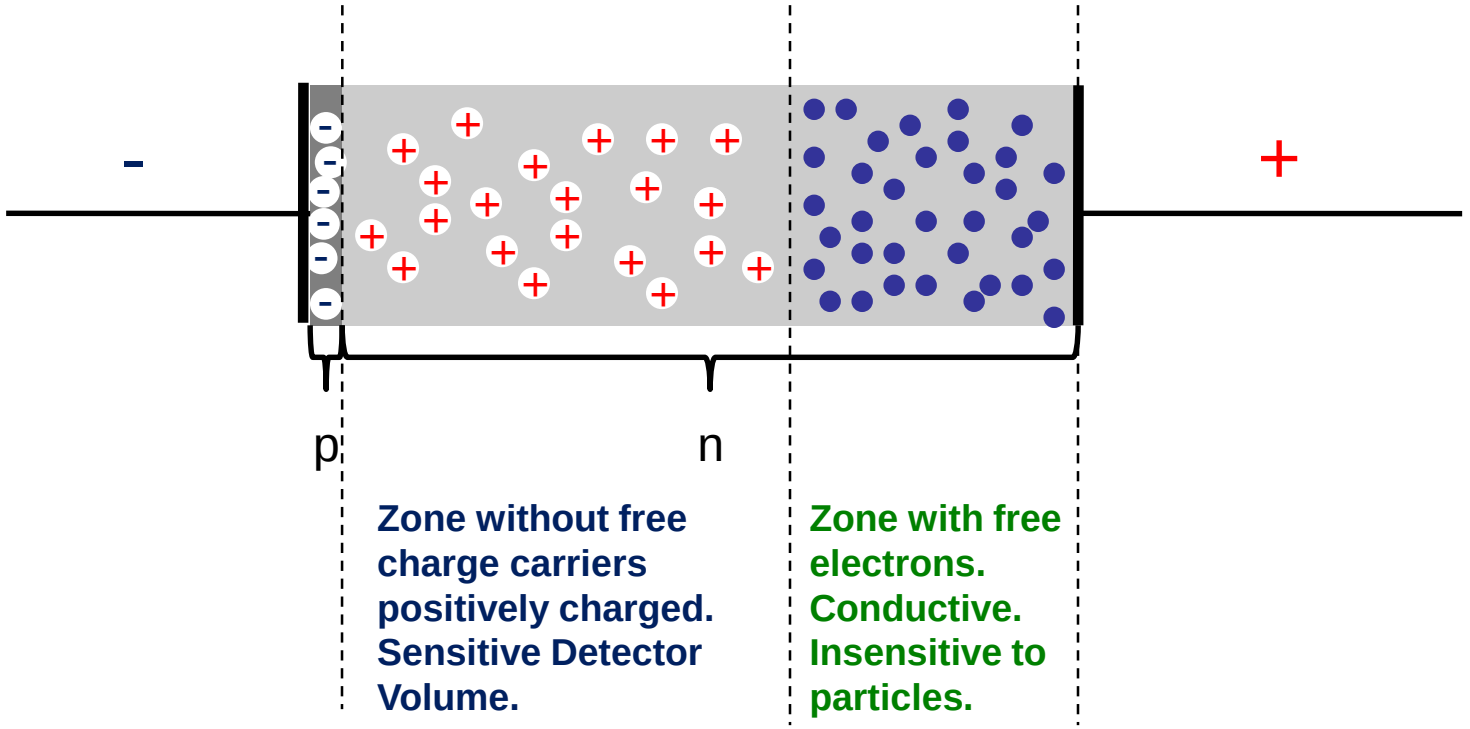

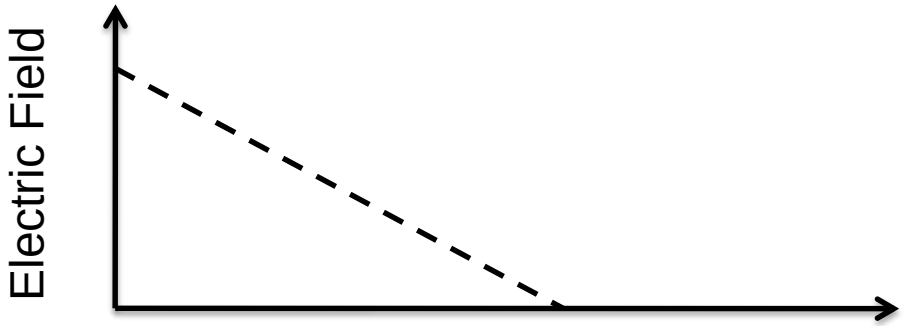

Fully-Depleted Silicon Detector

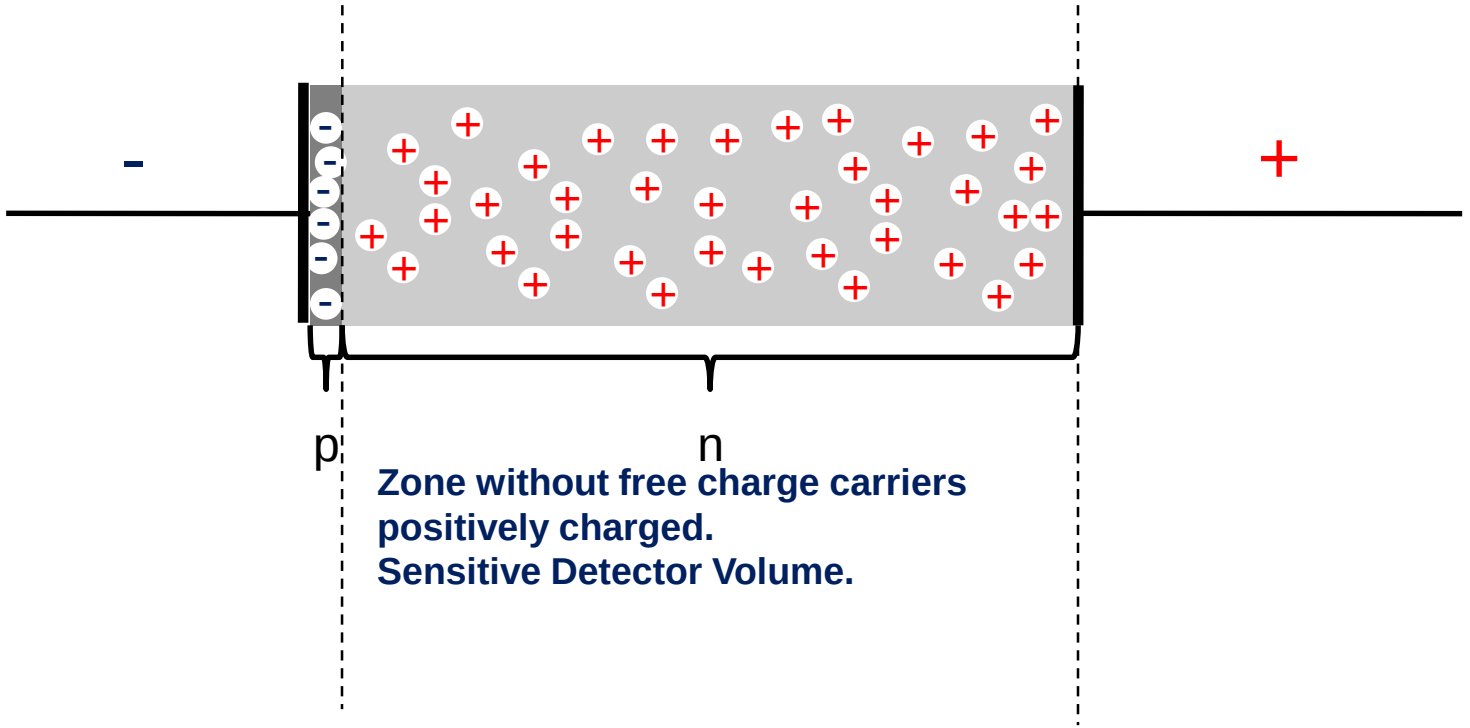

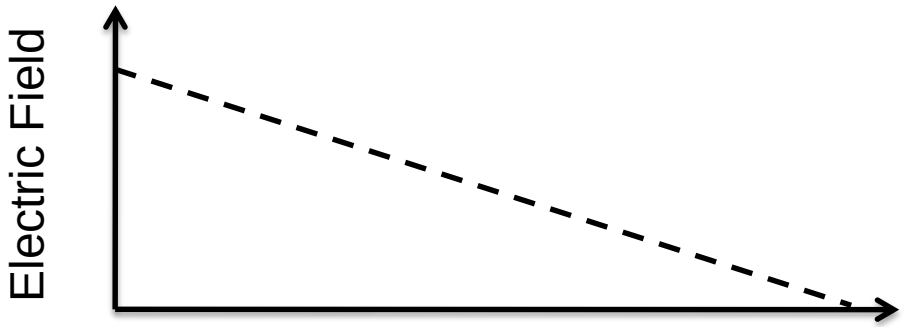

Over-Depleted Silicon Detector

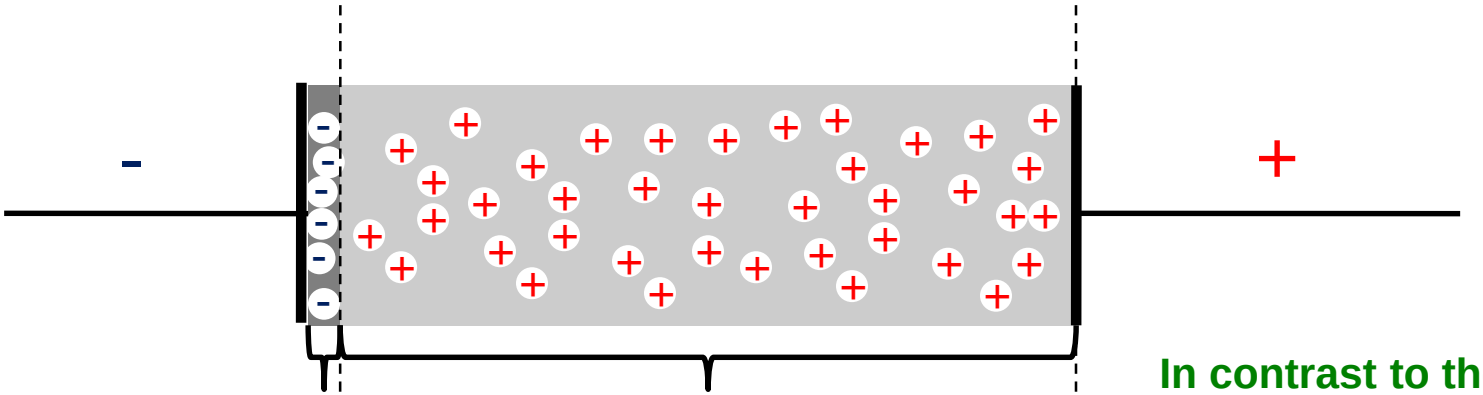

Zone without free charge carriers positively charged. Sensitive Detector Volume.

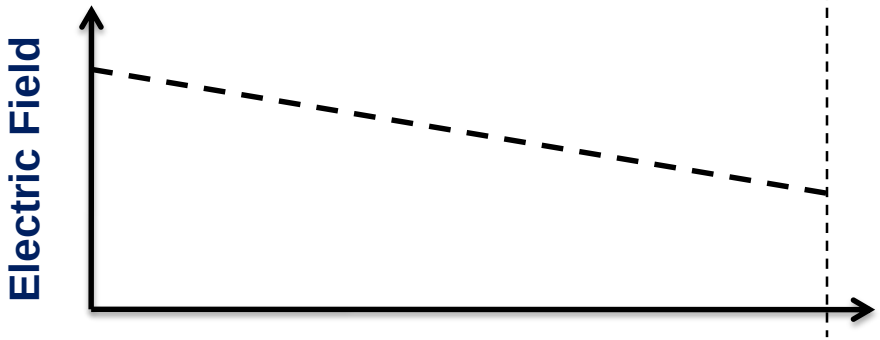

In contrast to the (un-doped) diamond detector where the bulk is neutral and the electric field is therefore constant, the sensitive volume of a doped silicon detector is charged (space charge region) and the field is therefore changing along the detector.

→ Velocity of electrons and holes is not constant along the detector.

Silicon Detector

Fully depleted zone

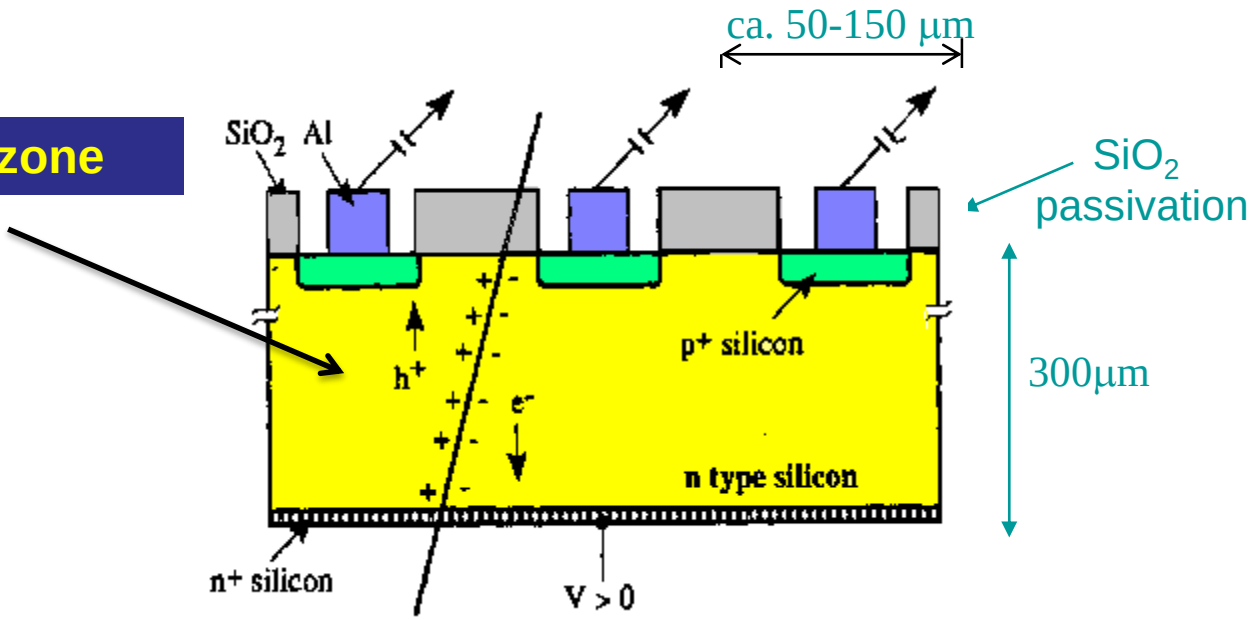

N (e-h) = 11 000/100μm

Position Resolution down to ~ 5μm !

Silicon Detector

Every electrode is connected to an amplifier →
Highly integrated readout electronics.

Two dimensional readout is possible.

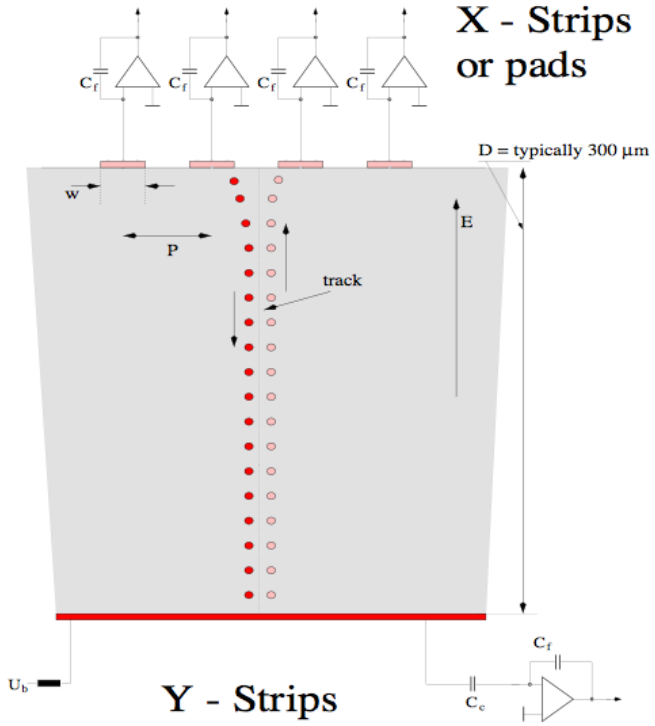

CMS Outer Barrel Module

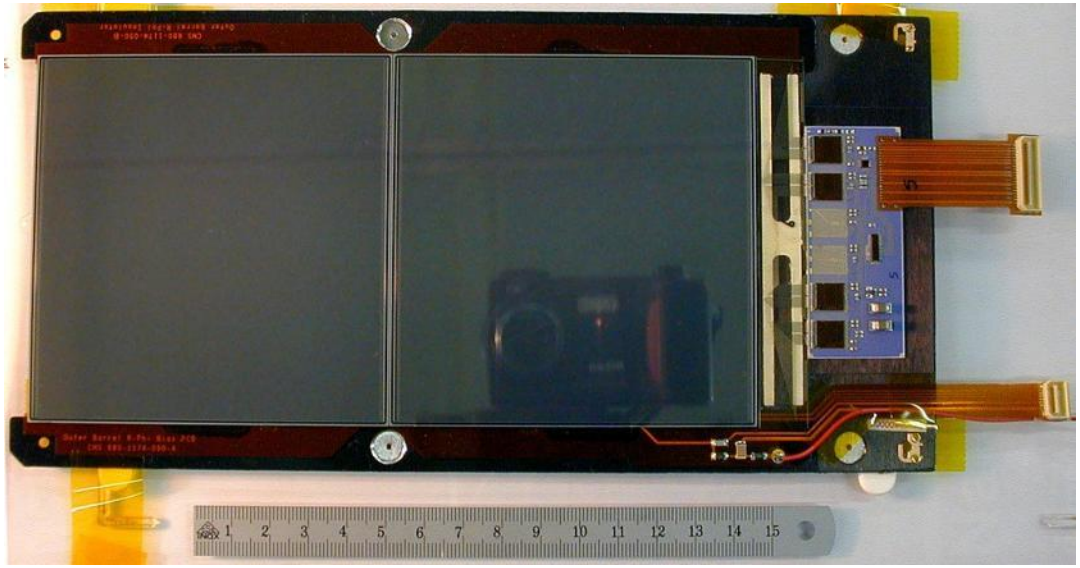

Large Silicon Systems

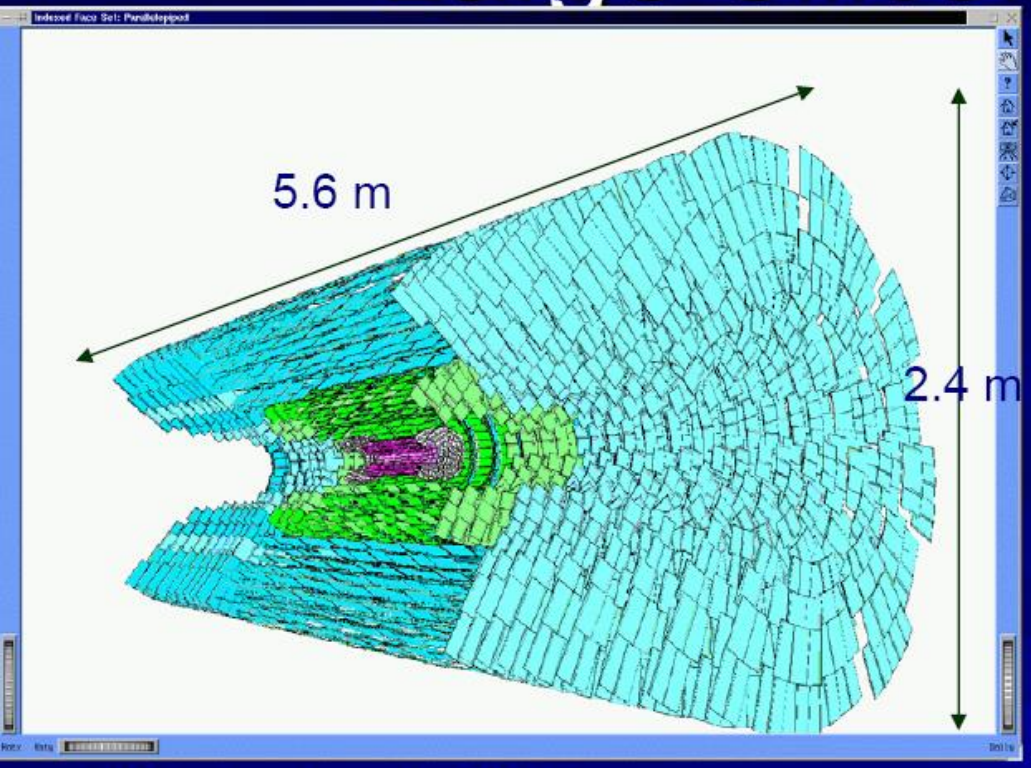

CMS tracker (~2007)

12000 modules

~ 445 m^2 silicon area

~ 24,328 silicon wafers

~ 60 M readout channels

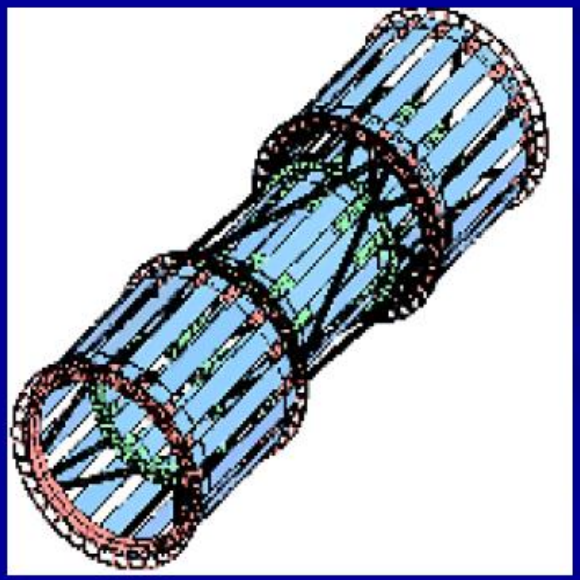

CDF SVX IIa (2001-)

~ 11m^2 silicon area

~ 750 000 readout channels

CMS Tracker

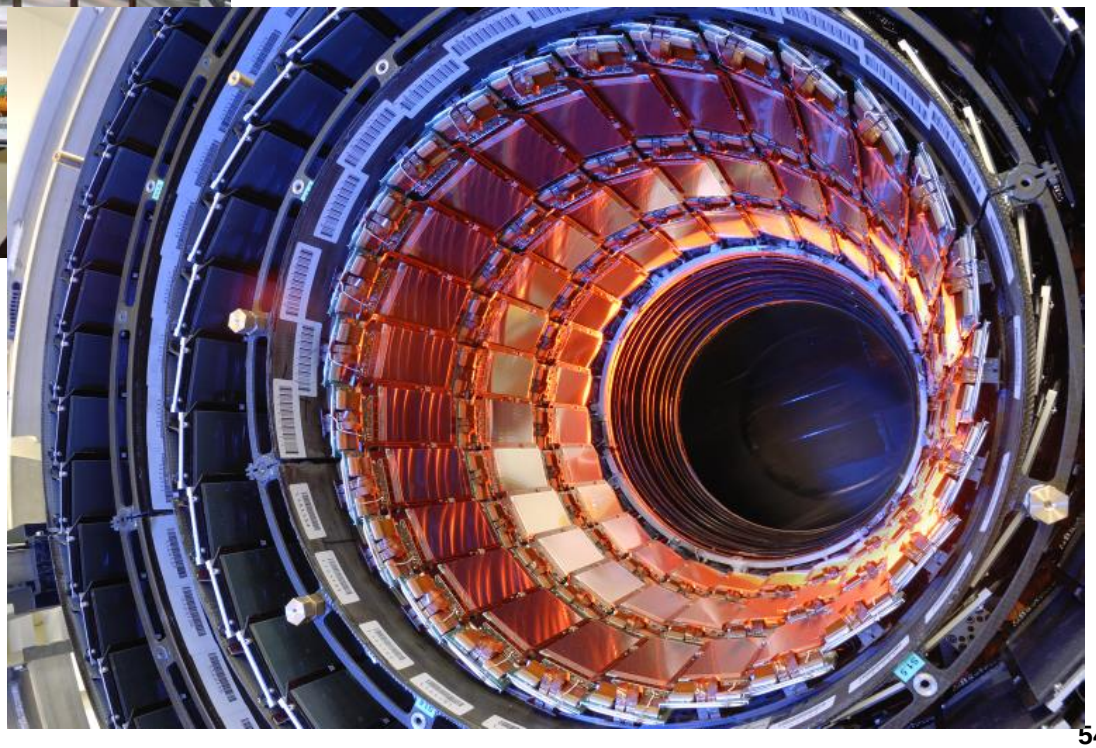

Pixel-Detectors

Problem:
2-dimensional readout of strip detectors results in ‘Ghost Tracks’ at high particle multiplicities i.e. many particles at the same time.

Solution:
Si detectors with 2 dimensional ‘chessboard’ readout. Typical size 50 x 200 µm.

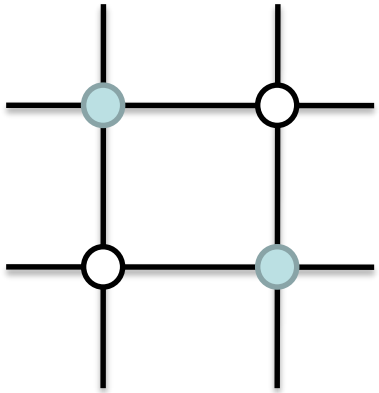

Problem:
Coupling of readout electronics to the detector

Solution:
Bump bonding

Bump Bonding of each Pixel Sensor to the Readout Electronics

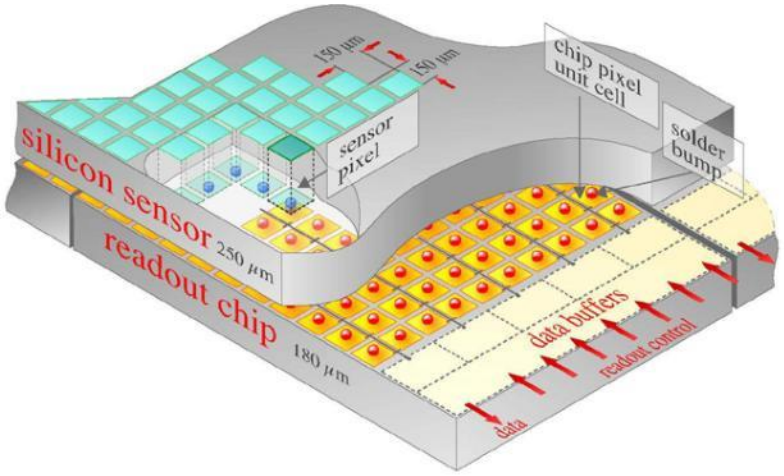

ATLAS: 1.4×10^8 pixels

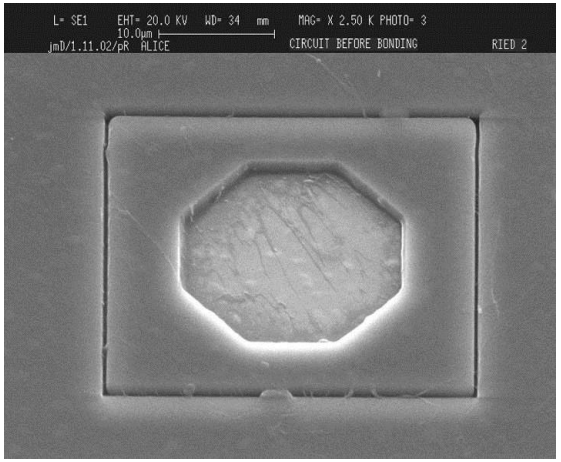

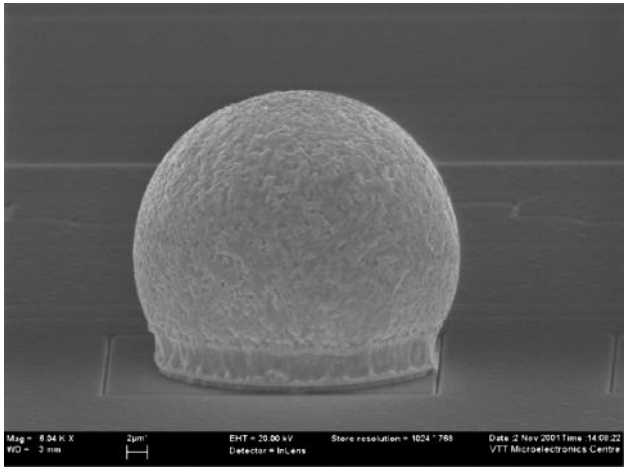

ATLAS Silicon Pixel Detector

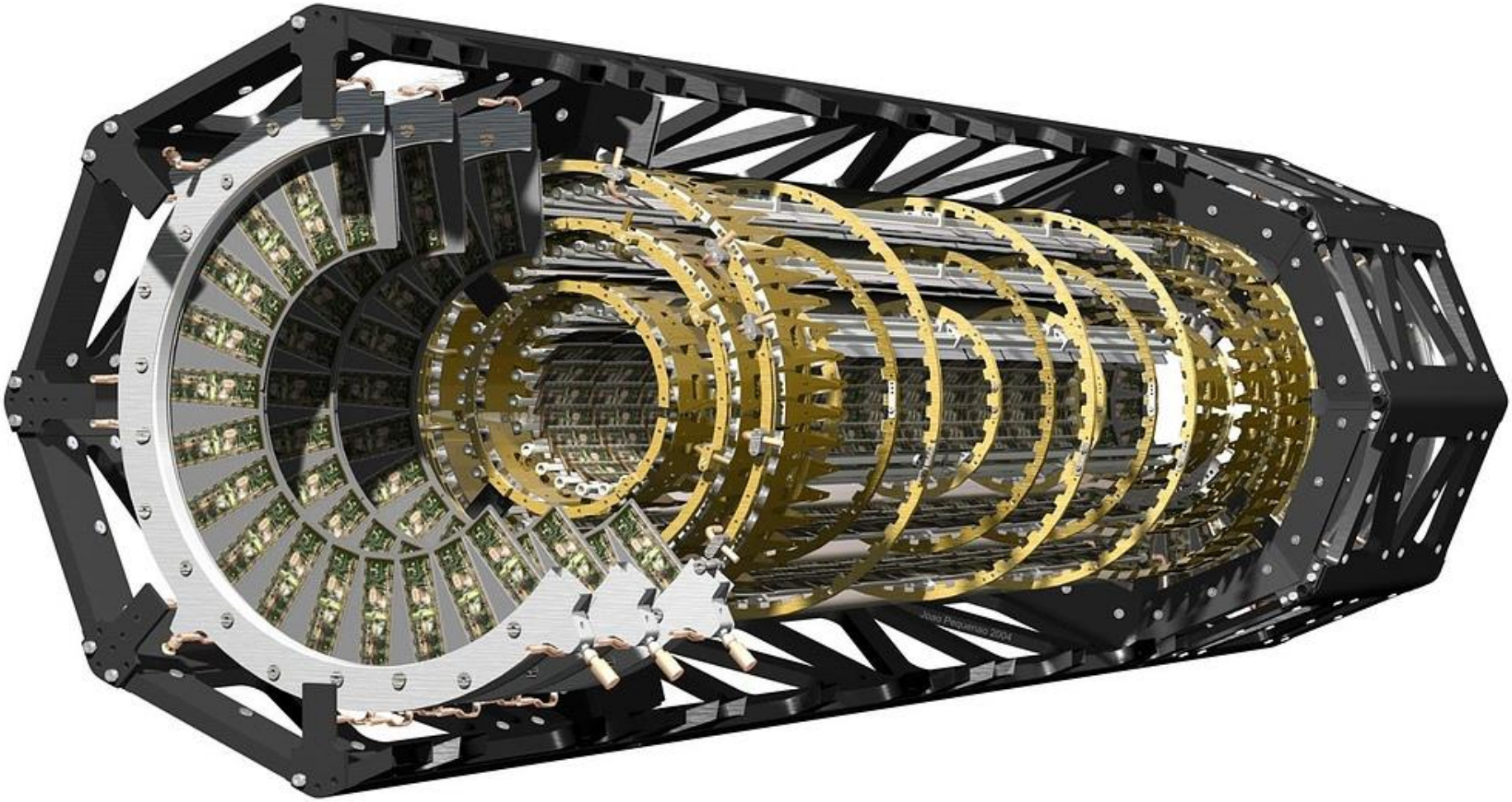

W. Riegler/CERN

Radiation Effects 'Aging'

Increase in leakage current

Increase in depletion voltage

Decrease in charge collection efficiency due to under-depletion and charge trapping.

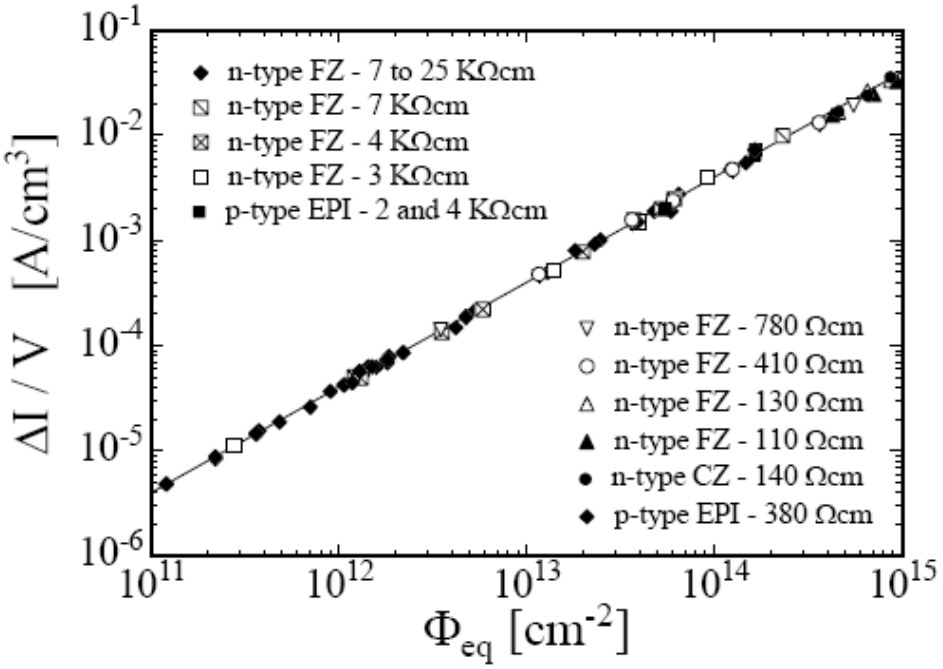

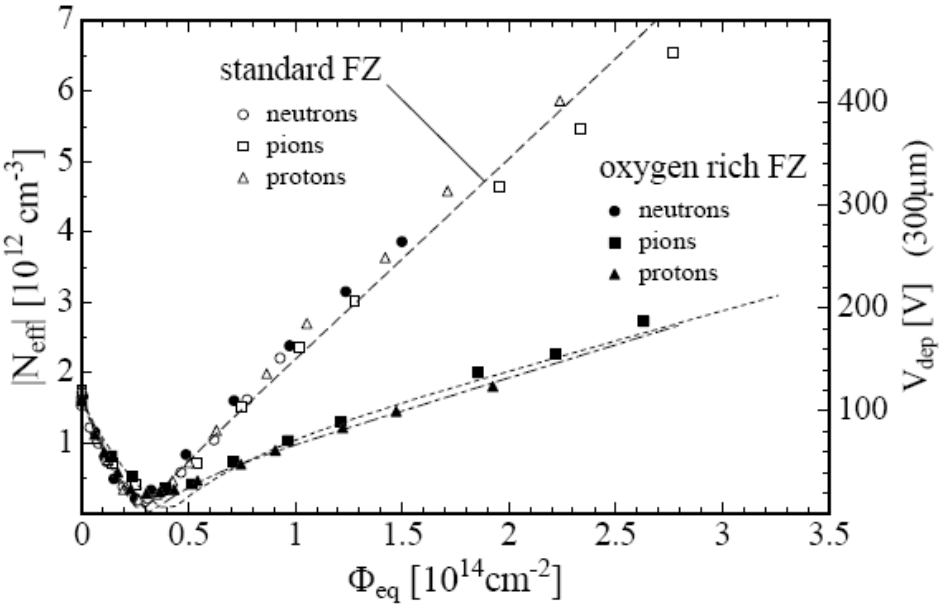

Obvious Goal: Monolithic Solid State Detectors
→Sensor and Readout Electronics as integral unit

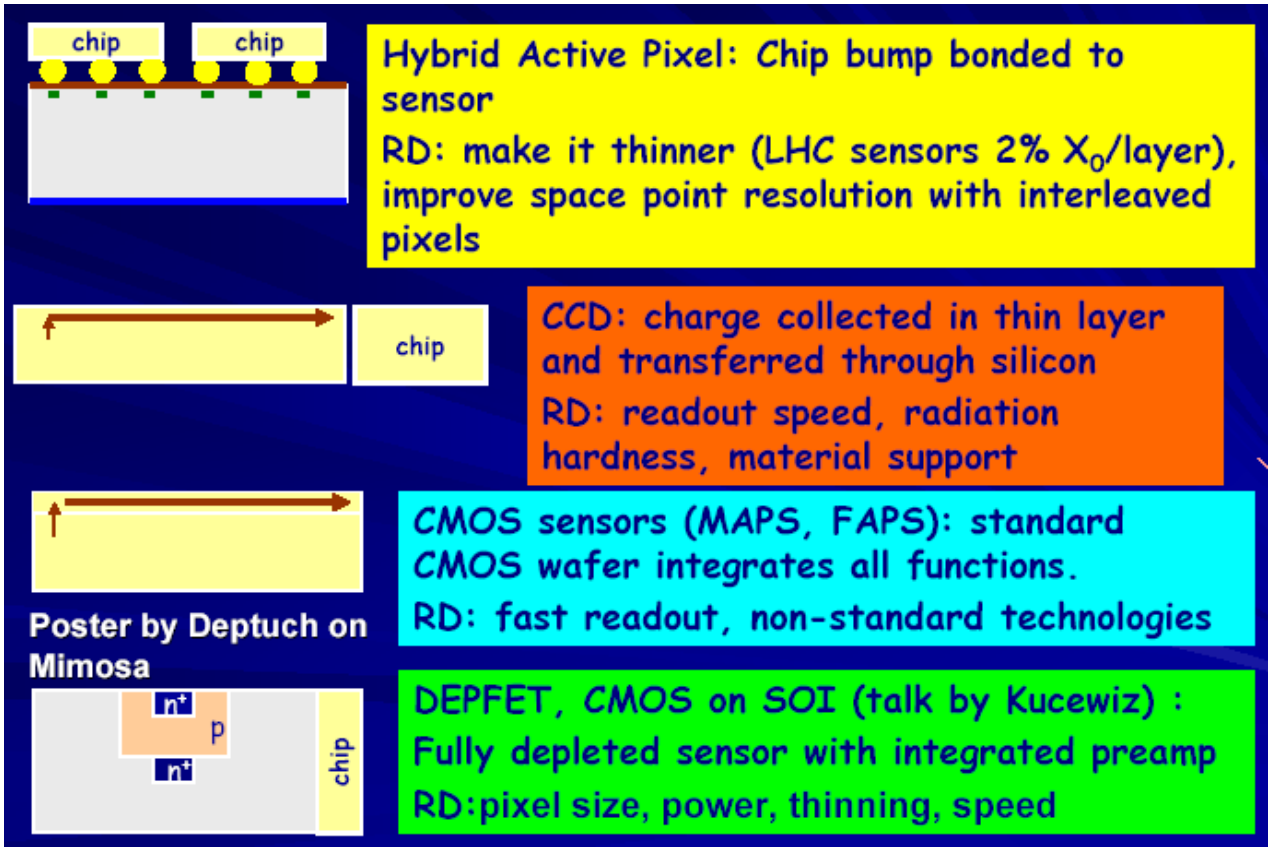

Large variety of monolithic pixel Detectors are explored, Currently mostly adapted to low collision rates of Linear Colliders.

Summary on Solid State Detectors

Solid state detectors provide very high precision tracking in particle physics experiments (down to 5um) for vertex measurement but also for momentum spectroscopy over large areas (CMS).

Technology is improving rapidly due to rapid Silicon development for electronics industry.

Typical numbers where detectors start to strongly degrade are 10^{14}-10^{15} hadron/cm^2.

Diamond, engineered Silicon and novel geometries provide higher radiation resistance.

Clearly, monolithic solid state detectors are the ultimate goal. Current developments along these lines are useful for low rate applications.

Calorimetry

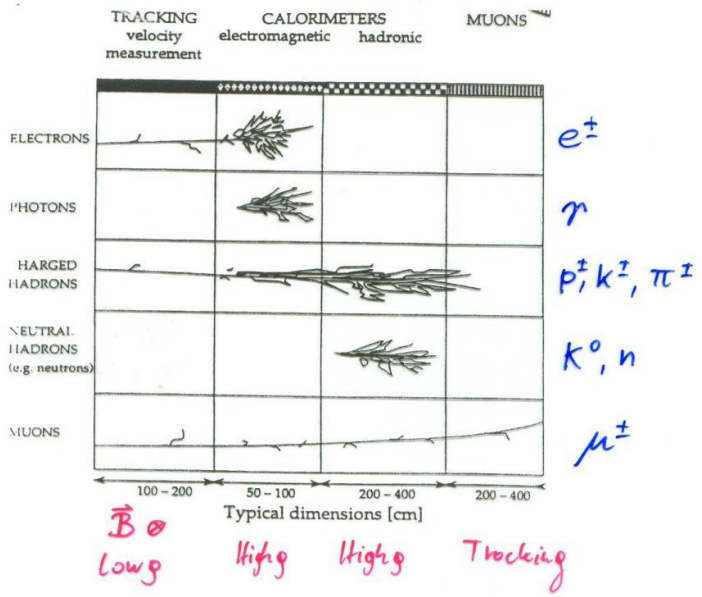

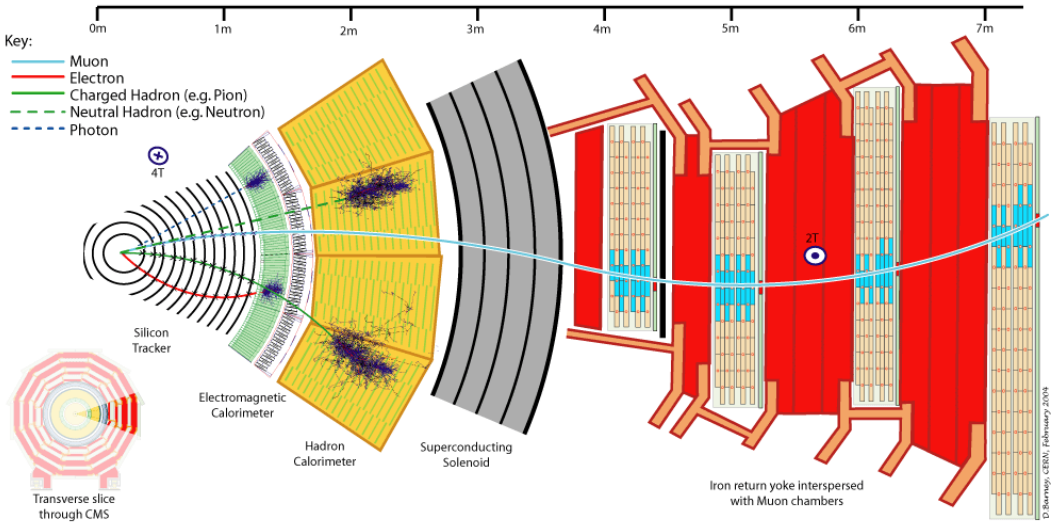

Calorimetry: Energy Measurement by total Absorption of Particles

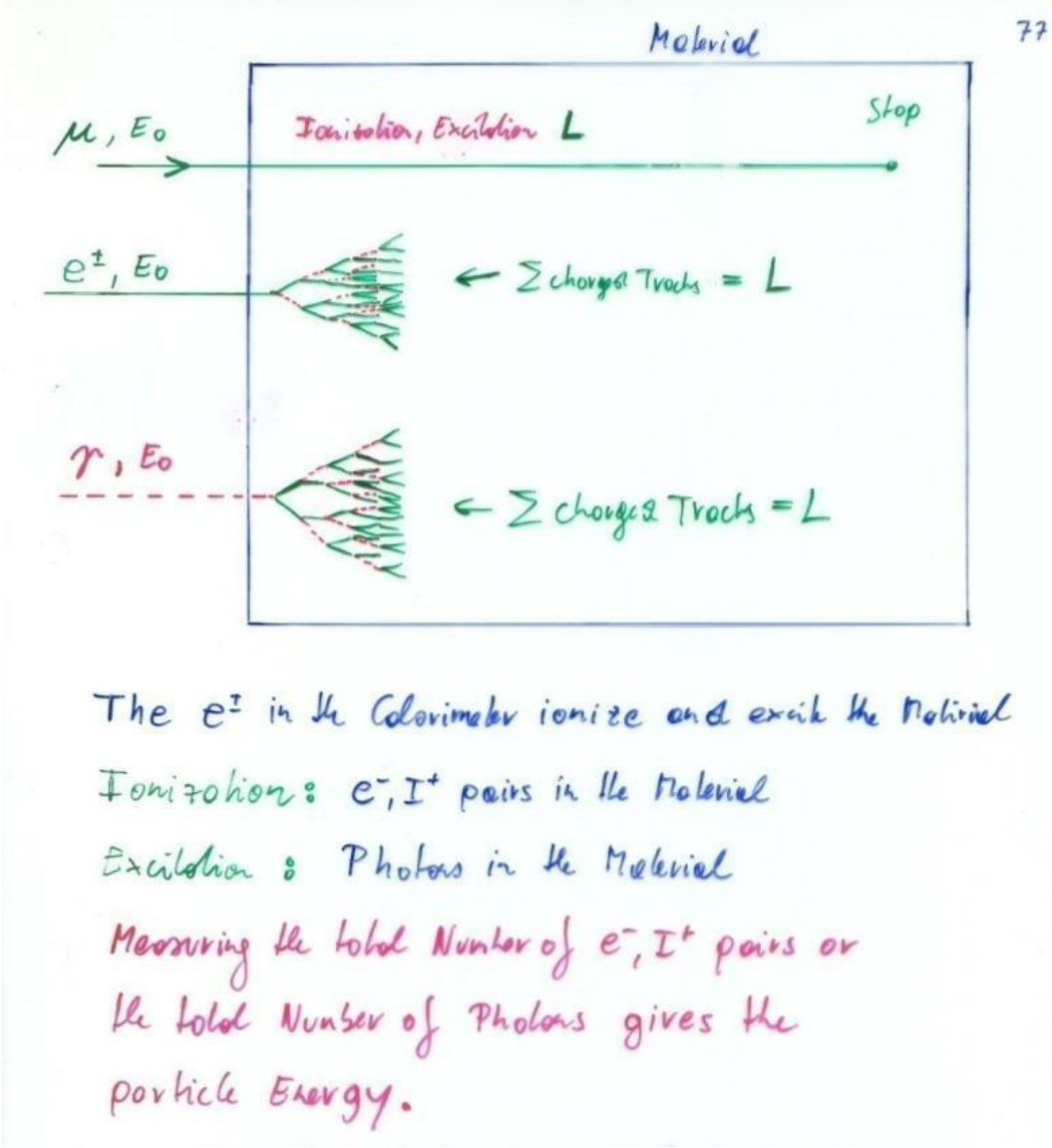

If N is the total Number of e^+, I^+ pairs or photons, or $N = c_1 E_0$:

$\Delta N = \sqrt{N}$ (Poisson Statistics)

$$\frac{\Delta E}{E} = \frac{\Delta N}{N} = \frac{1}{\sqrt{N}} = \frac{a}{\sqrt{E}} \rightarrow \text{Resolution}$$

Only Electrons and High Energy Photons show EM cascades at current GeV-TeV level Energies.

Strongly interacting particles like Pions, Kaons, produce hadonic showers in a similar fashion to the EM cascade →Hadronic calorimetry

Momentum Spectrometer: Δp/p α p

Calorimeter: Δ E/E α 1/ √ E

Energy measurement improves with higher particle energies – LHC !

Calorimetry: Energy Measurement by total Absorption of Particles

The measurement is destructive. The particle can not be subject to further study.

Energy Measurement by

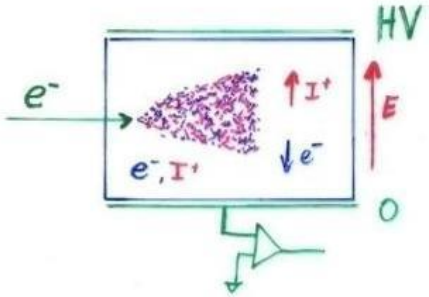

Collecting the produced Charge

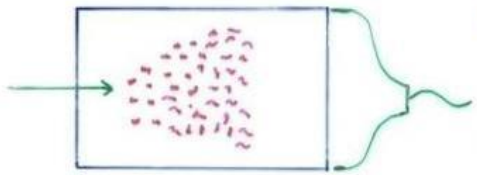

Measuring the Photons produced by the collision of the $e^{\pm}$ with Atom Electrons of the Material.

Total Amount of e^-, I^+ pairs or Photons is proportional to the total track length is proportional to the particle Energy.

Liquid Nobel Gases (Nobel Liquids)

Scintillating Crystals, Plastic Scintillators

Calorimetry

Calorimeters can be classified into:

Electromagnetic Calorimeters,
to measure electrons and photons through their EM interactions.

Hadron Calorimeters,
Used to measure hadrons through their strong and EM interactions.

The construction can be classified into:

Homogeneous Calorimeters,
that are built of only one type of material that performs both tasks, energy degradation and signal generation.

Sampling Calorimeters,
that consist of alternating layers of an absorber, a dense material used to degrade the energy of the incident particle, and an active medium that provides the detectable signal.

C.W. Fabjan and F. Gianotti, Rev. Mod. Phys., Vol. 75, N0. 4, October 2003

EM Calorimetry

Approximate longitudinal shower development

$N(n) = 2^n$ .... Number of particles ($e^\pm, \gamma$) after $n X_0$

$E(n) = \frac{E_0}{2^n}$ .... Average Energy of particles after $n X_0$

Shower stops if $E(n) = E_{critical}$

$\rightarrow n_{max} = \frac{1}{\ln 2} \ln \frac{E_0}{E_c}$ $\rightarrow$ Shower length rises with $\ln E_0$

Radiation Length X_0 and Moliere Radius are two key parameters for choice of calorimeter materials

Approximate transverse shower development

The transverse Shower Dimension is mainly related to the Multiple scattering of the low Energy Electrons.

$$\theta_0 \sim \frac{21\,[\text{MeV}]}{\beta p\,[\frac{\text{MeV}}{c}]} z_1 \cdot \sqrt{\frac{x}{X_0}}$$

Electrons E_c , $E \sim p \cdot c$

$$\theta_0 \sim \frac{21\,[\text{MeV}]}{\beta E_c\,[\text{MeV}]} \cdot z_1 \cdot \sqrt{\frac{x}{X_0}} \qquad z_1 = 1,\ \beta \sim 1$$

$$E_c \sim \frac{610}{Z+1.24}\ \text{MeV} \sim \frac{610}{Z}\ \text{MeV}$$

$$\theta_0 = 0.0344 \cdot Z \cdot \sqrt{\frac{x}{X_0}}$$

Moliere Radius ρ_m = lateral Shower Radius after $1 X_0$:

$$\rho_m \approx 0.0344 \cdot Z \cdot X_0$$

95% of Energy are in a Cylinder of $2\rho_m$ Radius.

Crystals for Homogeneous EM Calorimetry

In crystals the light emission is related to the crystal structure of the material. Incident charged particles create electron-hole pairs and photons are emitted when electrons return to the valence band.

The incident electron or photon is completely absorbed and the produced amount of light, which is reflected through the transparent crystal, is measured by photomultipliers or solid state photon detectors.

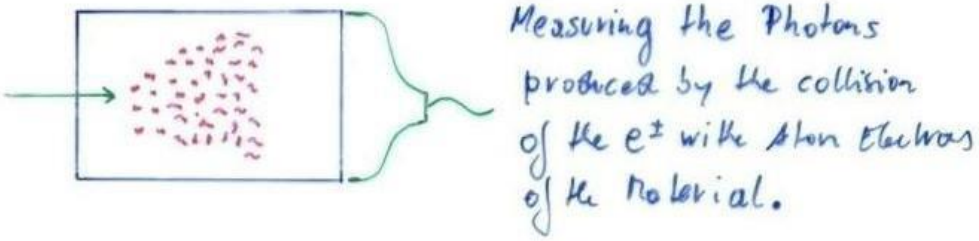

Crystals for Homogeneous EM Calorimetry

	NaI(Tl)	CsI(Tl)	CsI	BGO	$PbWO_4$
Density (g/cm^3)	3.67	4.53	4.53	7.13	8.28
X_0 (cm)	2.59	1.85	1.85	1.12	0.89
R_M (cm)	4.5	3.8	3.8	2.4	2.2
Decay time (ns)	250	1000	10	300	5
slow component			36		15
Emission peak (nm)	410	565	305	410	440
slow component			480		
Light yield γ/MeV	4×10^4	5×10^4	4×10^4	8×10^3	1.5×10^2
Photoelectron yield (relative to NaI)	1	0.4	0.1	0.15	0.01
Rad. hardness (Gy)	1	10	10^3	1	10^5

Barbar@PEPII, 10ms interaction rate, good light yield, good S/N

KTeV@Tevatron, High rate, Good resolution

L3@LEP, 25us bunch crossing, Low radiation dose

CMS@LHC, 25ns bunch crossing, high radiation dose

Crystals for Homogeneous EM Calorimetry

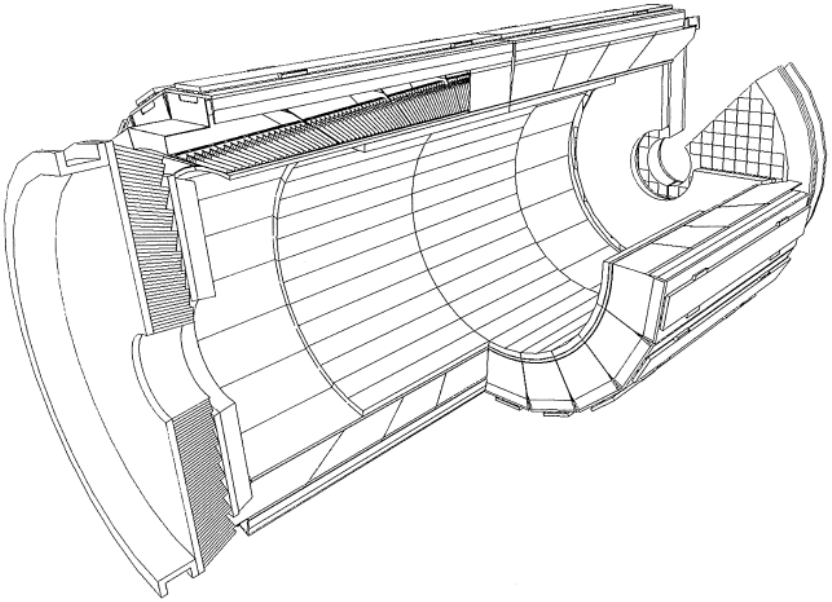

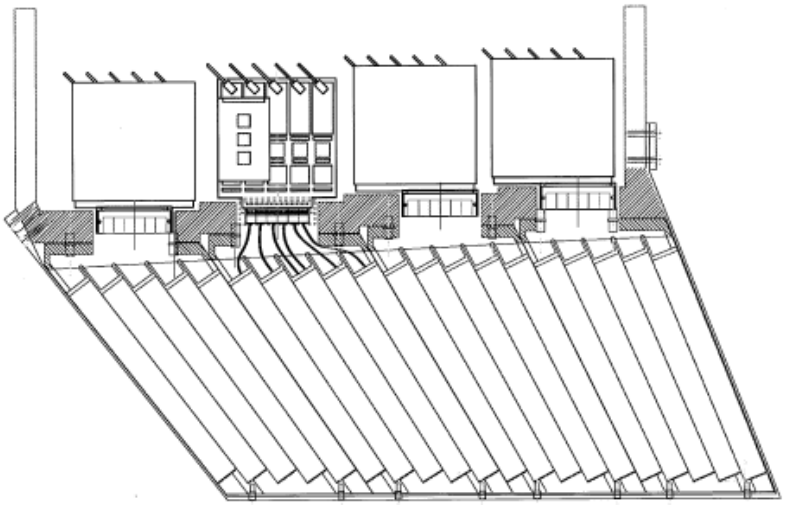

Fig. 2. Longitudinal drawing of module 2, showing the structure and the front-end electronics layout.

Noble Liquids for Homogeneous EM Calorimetry

	Ar	Kr	Xe
Z	18	36	58
A	40	84	131
X_0 (cm)	14	4.7	2.8
R_M (cm)	7.2	4.7	4.2
Density (g/cm^3)	1.4	2.5	3.0
Ionization energy (eV/pair)	23.3	20.5	15.6
Critical energy ϵ (MeV)	41.7	21.5	14.5
Drift velocity at saturation (mm/μs)	10	5	3

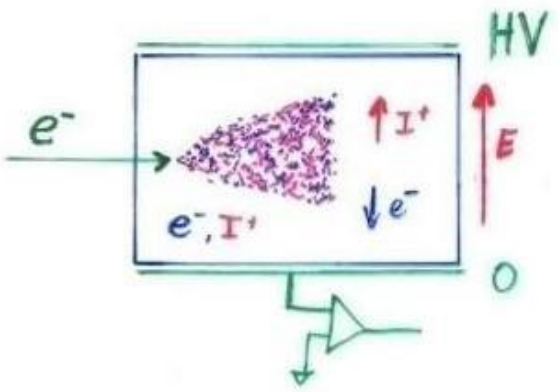

When a charge particle traverses these materials, about half the lost energy is converted into ionization and half into scintillation.

The best energy resolution would obviously be obtained by collecting both the charge and light signal. This is however rarely done because of the technical difficulties to extract light and charge in the same instrument.

Krypton is preferred in homogeneous detectors due to small radiation length and therefore compact detectors. Liquid Argon is frequently used due to low cost and high purity in sampling calorimeters (see later).

Noble Liquids for Homogeneous EM Calorimetry

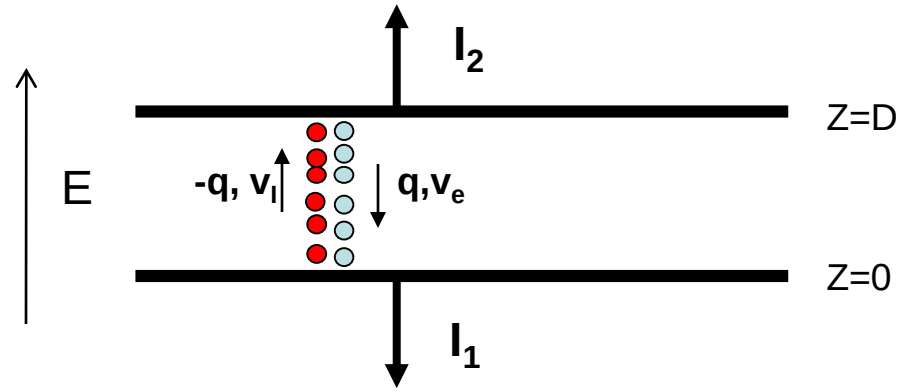

E.g. Liquid Argon, 5mm/ µs at 1kV/cm, 5mm gap → 1 µs for all electrons to reach the electrode.

The ion velocity is 10^3 to 10^5 times smaller → doesn't contribute to the signal for electronics of µs integration time.

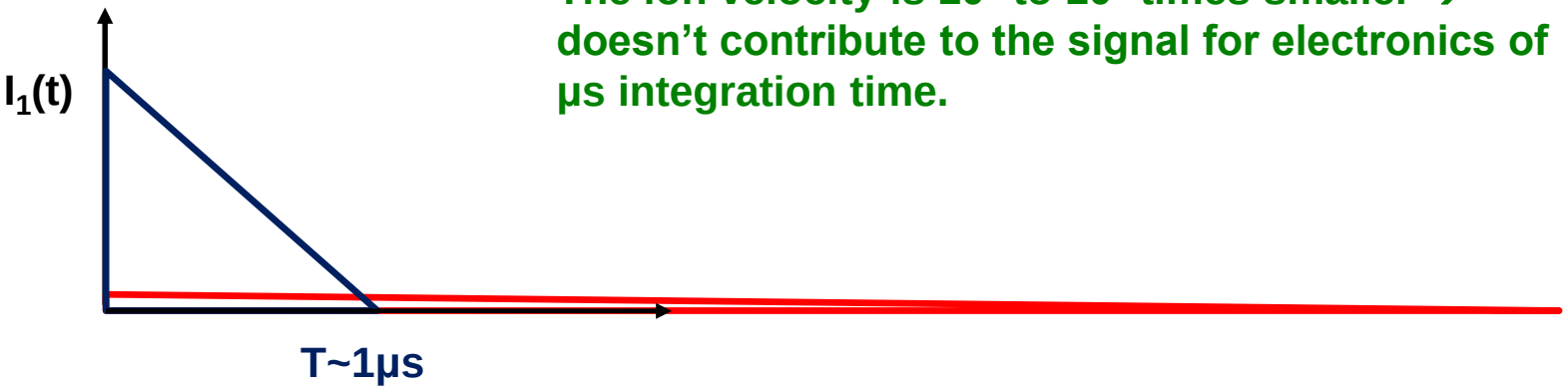

Homogeneous EM Calorimeters, Examples

NA48 Liquid Krypton
2cmx2cm cells
X_0 = 4.7cm
125cm length ($27X_0$)
ρ = 5.5cm

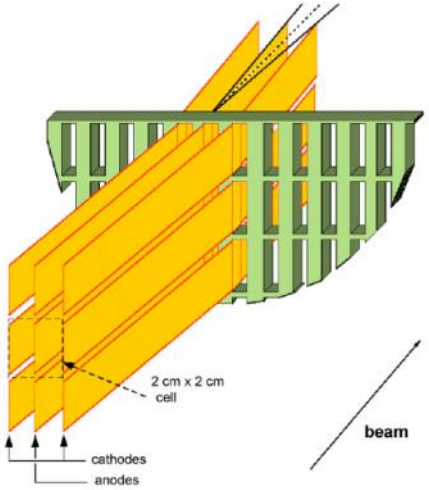

KTeV CsI
5cmx5cm and
X_0 = 1.85cm
2.5cmx2.5cm crystals
50cm length ($27X_0$)
ρ = 3.5cm

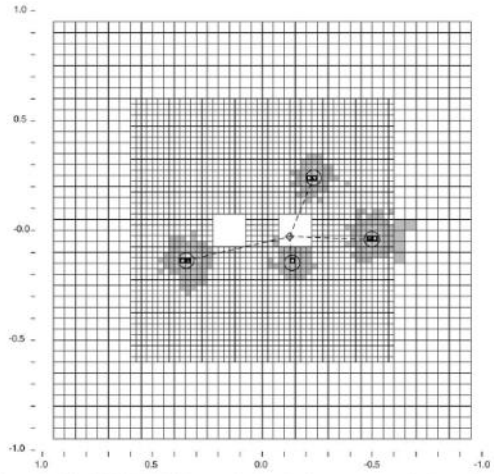

Fig. 1. Schematic of the KTeV CsI Calorimeter showing the cluster energy profiles due to four photons.

NA48 Experiment at CERN and KTeV Experiment at Fermilab, both built for measurement of direct CP violation. Homogenous calorimeters with Liquid Krypton (NA48) and CsI (KTeV). Excellent and very similar resolution.

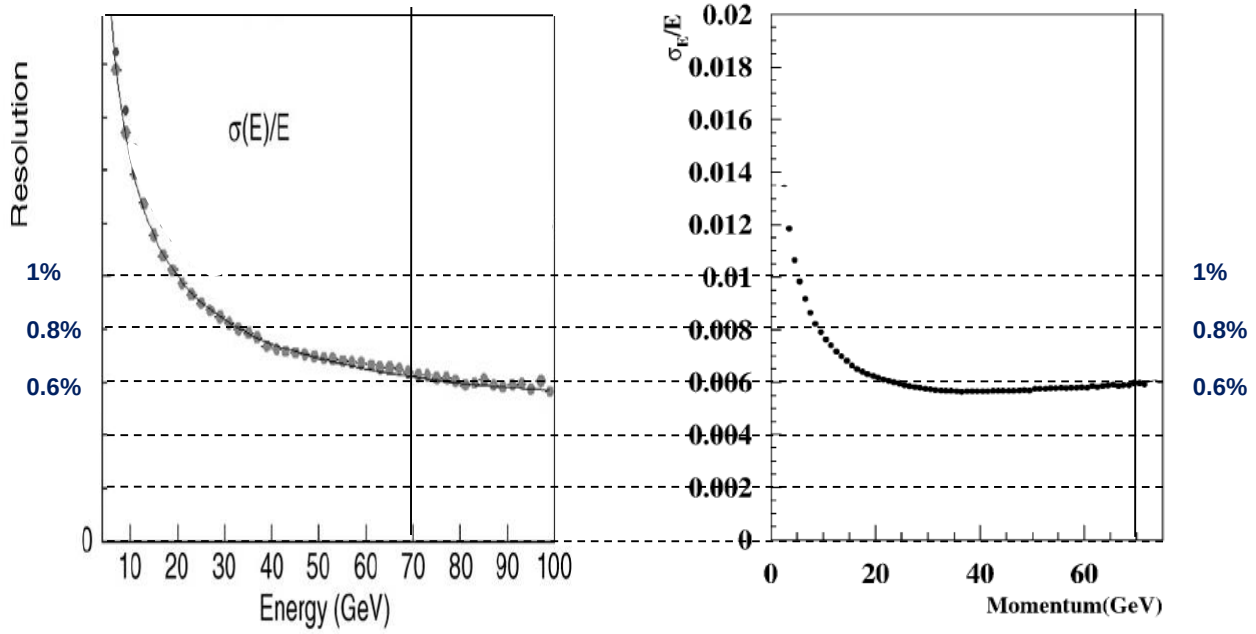

Sampling Calorimeters

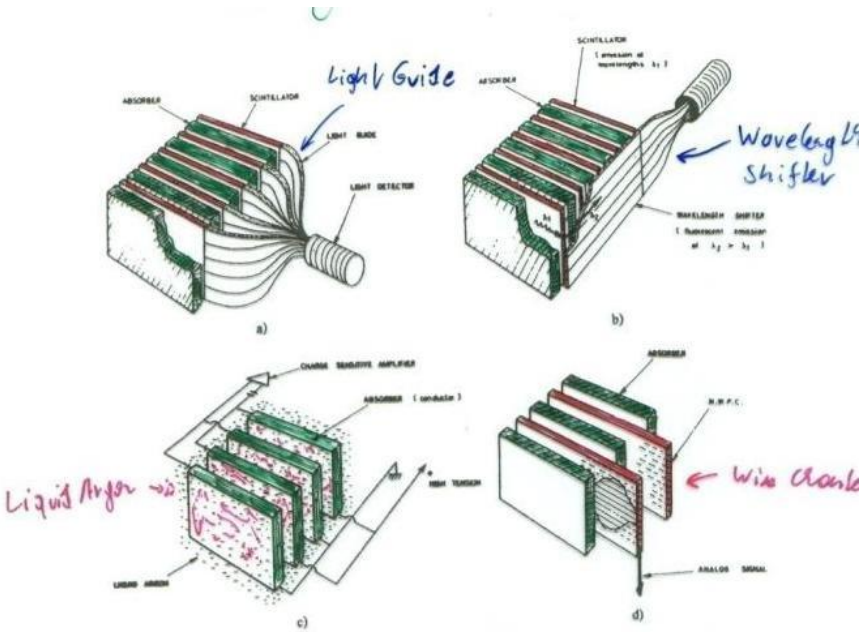

Alternation of "passive" absorber plates and "active" readout sections

Advantage:
- optimum choice of Absorber Material
- optimum choice of Signal Readout
- Compact and cheap Construction

"passive": Pb, Fe ....

"active": Scintillator (Signal → Photons)
Noble Liquid, e.g. Ar (Signal → e^-, I^+)
Wire Chambers (Signal → e^-, I^+)

Energy resolution of sampling calorimeters is in general worse than that of homogeneous calorimeters, owing to the sampling fluctuations – the fluctuation of ratio of energy deposited in the active and passive material.

The resolution is typically in the range 5-20%/Sqrt[E(GeV)] for EM calorimeters. On the other hand they are relatively easy to segment longitudinally and laterally and therefore they usually offer better space resolution and particle identification than homogeneous calorimeters.

The active medium can be scintillators (organic), solid state detectors, gas detectors or liquids.

Sampling Fraction = Energy deposited in Active/Energy deposited in passive material.

Calorimetry

Calorimeters are attractive in our field for various reasons:

In contrast with magnet spectrometers, in which the momentum resolution deteriorates linearly with the particle momentum, on most cases the calorimeter energy resolution improves as 1/Sqrt(E), where E is the energy of the incident particle. Therefore calorimeters are very well suited for high-energy physics experiments.

In contrast to magnet spectrometers, calorimeters are sensitive to all types of particles, charged and neutral. They can even provide indirect detection of neutrinos and their energy through a measurement of the event missing energy.

Calorimeters are commonly used for trigger purposes since they can provide fast signals that are easy to process and interpret.

They are space and therefore cost effective. Because the shower length increases only logarithmically with energy, the detector thickness needs to increase only logarithmically with the energy of the particles. In contrast for a fixed momentum resolution, the bending power BL^2 of a magnetic spectrometer must increase linearly with the particle momentum.

C.W. Fabjan and F. Gianotti, Rev. Mod. Phys., Vol. 75, N0. 4, October 2003